# 國 立 交 通 大 學

## 電子工程學系電子研究所

## 博 士 論 文

多人無線近身網路系統

Multiuser Wireless Body Area Networks

研 究 生 ：程士恒

指導教授 ：黃經堯 博士

中華民國 一〇一 年 八 月

# 國 立 交 通 大 學

## 電子工程學系電子研究所

## 博 士 論 文

多人無線近身網路系統

Multiuser Wireless Body Area Networks

研 究 生：程士恒

指導教授 ：黃經堯 博士

中華民國 一〇一 年 八 月

# 多人無線近身網路系統

# Multiuser Wireless Body Area Networks

研 究 生 ：程士恒　　Student: ShihHeng Cheng

指導教授 ：黃經堯 博士　　Advisor: ChingYao Huang

國立交通大學

電子工程學系 電子研究所

博士論文

A Dissertation
Submitted to Department of Electronics Engineering and
Institute of Electronics
College of Electrical and Computer Engineering
National Chiao Tung University
in partial Fulfillment of the Requirements
for the Degree of
Doctor of Philosophy
in

Electronics Engineering

Aug 2012

Hsinchu, Taiwan, Republic of China

中華民國 一〇一 年 八 月

# 多人無線近身網路系統

研 究 生 ：程士恒　　指導教授 ：黃經堯 博士

國 立 交 通 大 學
電 子 工 程 學 系 電 子 研 究 所

## 摘要

無線近身網路可利用短距離之無線傳輸擷取並傳送人體之重要生理資訊。其目前已被視為實現遠距照護(無遠弗屆醫療照護)之最重要的”最後一公尺”。無線近身網路其架構可以相當多元。透過適當的假設，無線近身網路可被比喻為”個人化之感測網路(personal sensor network)”、”社群用之隨意網路(social ad-hoc network)”、或是”醫療用之網狀網路(medical-specific mesh network)”。也因此目前許多既有之感測、隨意、與網狀網路之技術可用來增進無線近身網路之效能。本研究進一步探討無線近身網路特有之”近身網路間干擾”議題。此議題來自於無線近身網路使用者之移動性。經常性的近身網路移動所導致之彼此重疊或碰撞造成無線節點密度之劇烈變化，因此引發劇烈之近身網路間互相干擾而導致傳輸效能與可靠性之低落。透過建立多近身網路使用者之干擾模型，本研究率先指出近身無線網路之設計挑戰。其包含: 1) 在高密度近身網路情境下，如何同時增進網路使用效能與快速反應因使用者移動性所帶來之拓樸與干擾變化?(以傳統圖學資源分配觀點來看，此兩校能參數互為取捨) 2) 如何在多使用者近身網路中建立洽當之優先權制度?此制度須同時考量感測器類別、

使用者狀態、與緊急事件總類等之個別差異性。 3)如何在分散式網路的架構下實現以上需求? 在本論文中，我們針對各議題做深入討論並提供其個別的解決方案，包含隨機非完整著色法(Random Incomplete Coloring)用來最大化無線近身網路資源分配之速度與頻道利用效率與隨機資源競爭(RACOON)演算法用來實作分散式近身網路之優先權制度。其個別效能探討將搭配相關理論模型與電腦實驗。

**關鍵字： 無線近身網路，感測器，低功耗，頻道效益，品質服務(QoS)，媒體接取控制，資源分配，著色理論。**

# Multiuser Wireless Body Area Networks

Student: ShihHeng Cheng Advisor: Dr. ChingYao Huang

Department of Electronics Engineering and
Institute of Electronics
National Chiao Tung University

## Abstract

Wireless Body Area Network (WBAN) is designed to retrieve important body signals through short range wireless technology in charge of the "last meter" of ubiquitous healthcare. With proper assumptions of network architecture, WBAN can be regarded as a "personal sensor network", a "social ad-hoc network", or a "medical-specific mesh network". Based on the experiences of these well-known wireless technologies (sensor, ad-hoc, and mesh networks), this study further discusses and puts more focus on effects of "inter-WBAN interference." This multi-WBAN-specific issue is caused by the mobility of WBAN users. When WBANs are moved with users, they frequently encounter and overlap with each other. These WBAN-overlaps lead to dramatic changes of sensor density and hence creates dynamic mutual interferences between WBANs. Through establishing interference models of multiuser WBANs, this study first identifies design challenges under the inter-WBAN interference. Primary challenges include 1) simultaneously improving channel efficiency in high density WBAN while maintaining fast response time to rapid WBAN topology changes (these two performance indexes are tradeoffs in term of traditional scheduling theory), 2) Constructing the proper priority scheme for multiuser

WBAN which can simultaneously satisfy priority requirements from sensor types, user conditions, and emergency-handling points of views, and 3) solving these problems in distributed WBAN systems. This study will discuss above issues in separate chapters. Corresponding solutions, Random Incomplete Coloring (RIC) and RACOON algorithms that solve speed-efficiency trade-offs of traditional coloring and WBAN-specific priority schemes, respectively, will be introduced. Improvement of related performance indexes will be carefully verified by proper analytical models and experiments.

**Keywords: Wireless Body Area Network, Sensors, Low Power, Channel Efficiency, Quality of Service (QoS), Medium Access Control, Resource Scheduling, Graph Coloring.**

# Acknowledgements

I would like to dedicate this work to my love, Karen, and my family.

I want to thank Prof. ChingYao Huang for all his valuable advices and supports of this study. I also want to thank National Chiao-Tung University (NCTU) and WanFang Hospital's U-PHI project team members who inspired me to combine medical and tele-healthcare experiences in my work. I want to specially thank Prof. Hung-Lin Fu for his advices to the math models constructed in this study. Finally, I appreciate all important suggestions from my dissertation committees that have helped complete this work.

# Contents

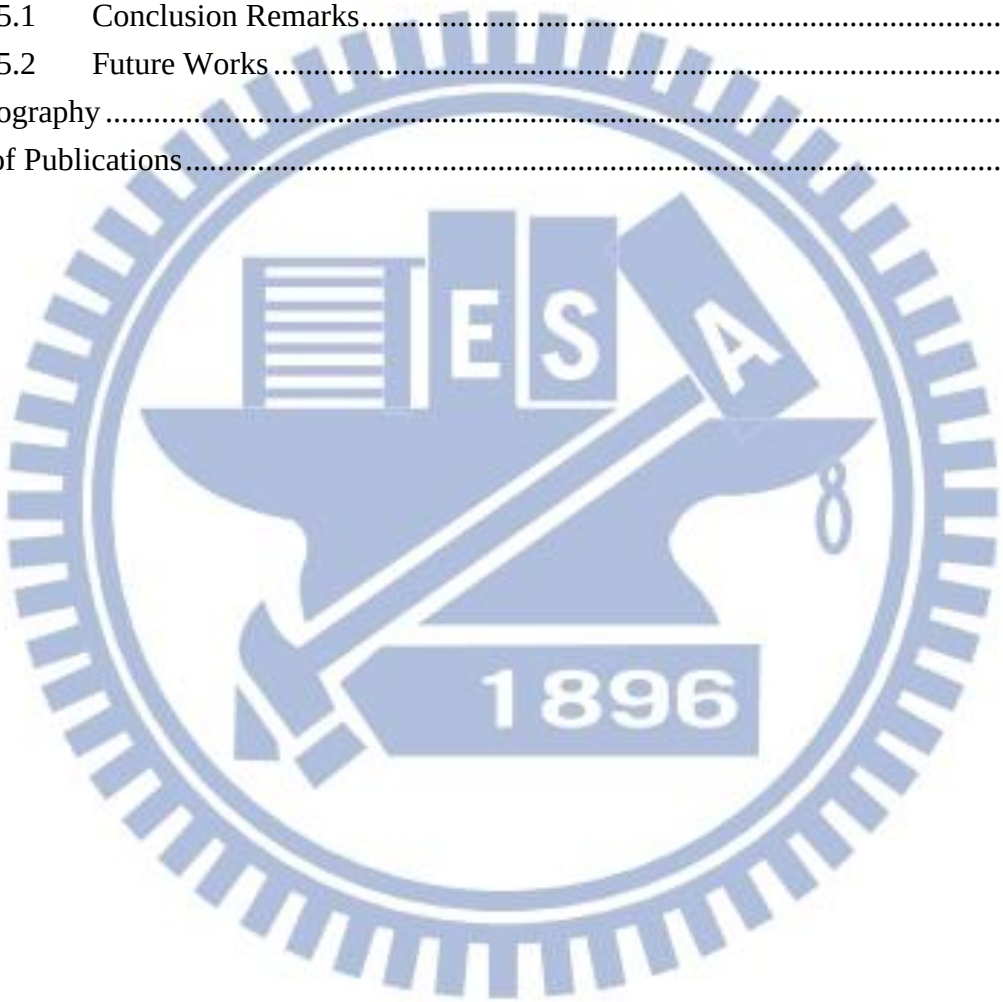

# List of Tables



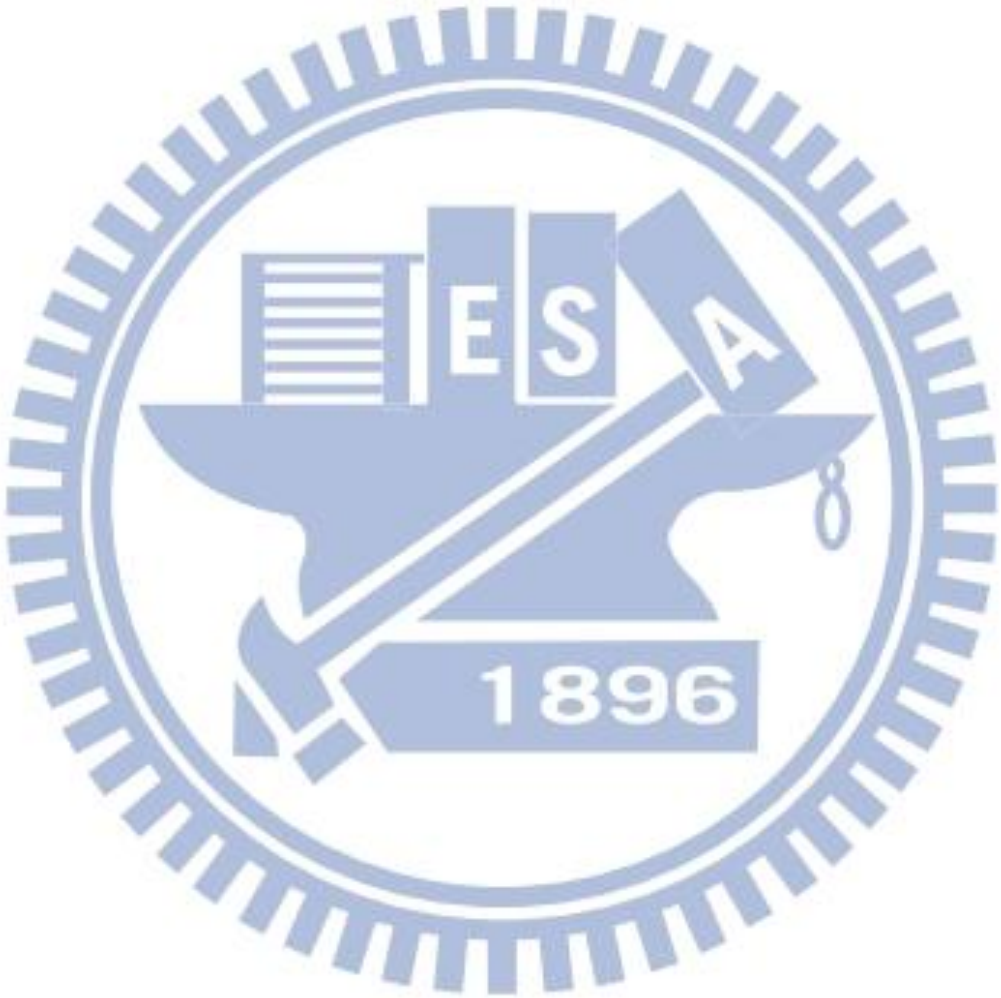

# List of Figures

# Chapter 1

# Introduction of Multiuser WBANs

Wireless Body Area Network (WBAN) is a short range communication (3~5 meters) which realizes ubiquitous health monitoring by breaking the wire-line limitation of traditional near/inner body signal measurements. WBAN bridges these "last meter" vital signals with hospital or clinics for further diagnosis and health tracking [1, 2]. As illustrated in **Fig.** 1-1, a single WBAN can be regarded as a "personal sensor network," formed by a group of wireless sensor nodes (WSNs) and a central processing node (CPN) that collects various vital signals from these WSNs. However, different from traditional sensor networks focused on static or low mobility scenarios [3], a WBAN has a higher moving speed[1] and more frequent topology changes due to user movement [2]. The moving topology of multiple WBANs is similar to that of mobile ad hoc networks (MANETs) [4], but with group-based rather than node-based movement. The "high mobility" and "group-based movement" differ the WBAN from a sensor network and a MANET. These properties of WBAN create a new research topic of inter-WBAN interaction, which includes new inter-WBAN interference and quality of services (QoS) issues. Hence, a WBAN-specific medium access control (MAC) is required. Before discussing design challenges of WBAN MAC, the network architecture of WBAN is introduced to specifically define the scope of this study.

1 A WBAN has "notable mobility" by considering its short transmission range (3~5meters) as compared with human moving speed (meters per second when walking or running).

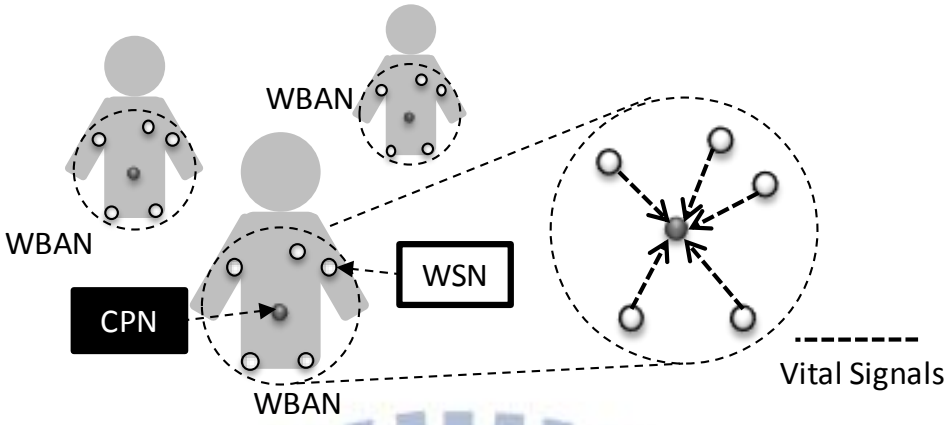


Fig. 1-1 Wireless body area networks (WBAN)

## 1.1 Network Architecture

To realize ubiquitous health monitoring, a general WBAN can incorporate many popular wireless technologies. According to combinations of different levels of WBAN architecture, a WBAN can be treated as a “personal sensor network”, a “social ad-hoc network”, or a “medical-specific mesh network”, as shown in Fig. 1-2. On the sensor level, each WSN can measure certain body information and forward it to CPN. While the scenario is extended to multiple WBANs, also known as the coordinator level, WBANs can share information with each other for social-application purposes. This network becomes a distributed ad-hoc network, formed through gathered WBAN users. The key of the ubiquitous health monitoring is the backbone level. On this level, remote hospitals or tele-healthcare center can receive the body signals collected by CPN through cellule systems.

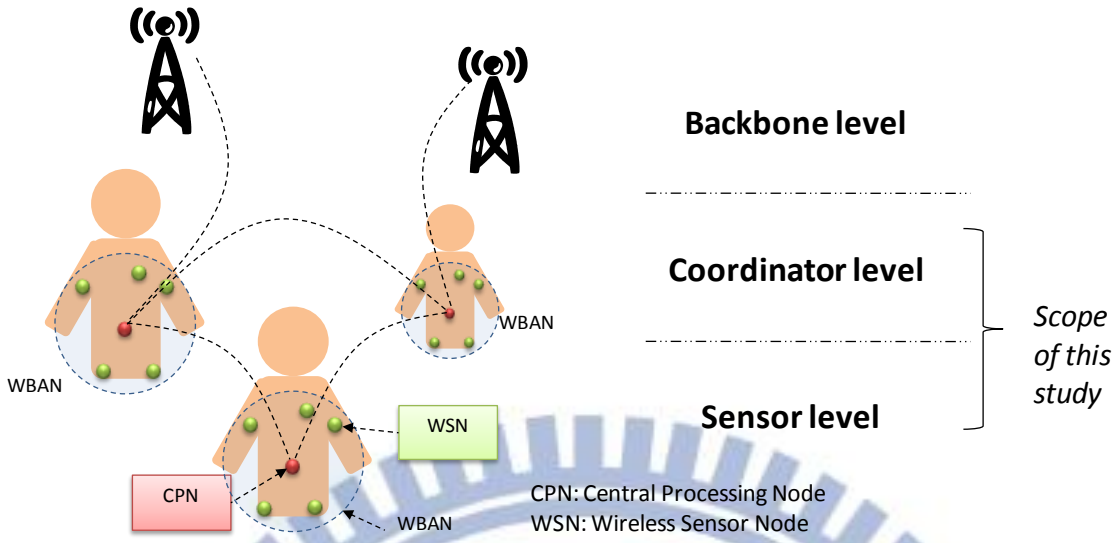


Fig. 1-2 General WBAN architectures

Many issues concerning general WBAN have been well studied, for example, power consumption optimization on the sensor level (for a single WBAN) and QoS control on the backbone level [5-7]. Also, experiences from related domains can provide direct or in-direct solutions for WBAN-related issues, for instance, ad-hoc scheduling for coordinator level WBAN [8-12]. However, there is a WBAN-specific issue still in need of further exploration, "inter-WBAN interference," which is also the topic of this study. This unique issue comes from the mobility of WBAN users. A group of sensors (including CPN and WSNs) are carried by a WBAN user. Groups (WBANs) encounter and overlap with each other when multiple WBAN users gather together. When wireless resources of WBANs are not proper interleaved, this generates problems of mutual interference between WBANs (sensor groups). To analyze this issue, this study focuses on the architecture in the coordinator and sensor levels with following assumptions:

- WBANs are fully distributed systems – There are no higher advanced coordinator than WBANs. Even if it were possible to share information between WBANs through a backbone system, due to the backbone latency, Backbone system may not be able to timely exchange

real-time information like mutual locations, network loading, and priorities between WBANs. These information are important for instant resource allocation between WBANs. Therefore, this study assumes that each WBAN can only share data with its neighbors that are within its communication range. Each WBAN performs this communication individually.

- Each WBAN has a simple-star topology – Each WBAN is formed by a CPN and a group of WSNs. Usually, WSNs are designed to have meters transmission range, which is larger than the normal size of a human body. Hence, this study assumes each CPN can directly access each WSN in a one-hope communication.

- CPN-based resource scheduling – This study adopts a CPN-based scheduling due to the imbalanced CPN/WSN architecture of a simple star (**Fig.** 1-1). In a single WBAN, the CPN plays the role of the master and the WSNs are the slaves. The CPN manages the join, leave, and functional-control of the WSNs. In contrast, WSNs are passive devices, which are designed to retrieve specific vital signals such as blood pressure or electrocardiograms (ECG) and forward them to the CPN. Additionally, a CPN is usually embedded in personal devices such as cellular phones or PDAs with larger and rechargeable batteries. Dissimilarly , a WSN is expected to be light weighted (small battery) and even non-rechargeable for certain implantable applications. These two unbalanced features suggest shifting power-consuming network controls from WSNs to the CPN. Therefore, for the inter WBAN scheduling. CPN represents its WBAN and negotiates wireless resources between WBANs. And then, for the intra WBAN scheduling, CPNs centrally allocates the wireless resources (reserved in the inter WBAN negotiation) to its WSNs based on their traffic loading and QoS requirements.

As a result, WSNs only function when receiving commands from CPNs and transmitting data in its allocated wireless resource to minimize power consumptions.

## 1.2 Design Challenges of Multi-User WBAN MAC

As mentioned, inter WBAN interference comes from the mobility of WBAN users. WBAN densities can vary when WBAN users are alone or in a crowded place. Mutual interferences between WBANs might seriously impact the channel efficiency in high density WBANs. This is the reason that IEEE 802.15 TG6, the standard task group of WBAN, requires that the WBAN protocol support at least the sensor density: 60 sensors in a $6^3 m^3$ space [13]. Furthermore, densities could change very rapidly in certain scenarios, before and after entering a crowded elevator for example. Therefore, improvements on maintaining high channel efficiency in crowded WBANs and conducting short response time to the density change of WBANs are major design targets of WBAN MAC. However, these two performance indexes are tradeoffs according to traditional coloring theory, an important theory for resource scheduling, and will thus be discussed in chapter 3).

Mutual interference also leads to complex priority issues in WBAN QoS designs. In each WBAN, WSNs may have difference priorities according to signals they collect. For example, the priority of ECG sensors might require higher priority than that of temperature sensors, since ECG sensor directly respond to life-threatening instances. Also, priorities of sensors may dynamically increase when abnormal signals are detected. This can ensure immediate triggering of related emergency procedure. In addition, priority definitions may various depending on the status of WBAN users. For example, the priority of the temperature of a user in fever may require higher priority than that of a healthy user. As a result, complex priority requirement is another major design challenge for multiuser WBAN MAC.

In this study, the impact of inter-WBAN interference will be first evaluated in chapter 2. Analytical throughput and energy consumption models are provided to point out the key of performance degradation. Chapter 3 further considers the rapid topology change of WBAN and discusses the tradeoff between fast-response-time and channel-efficiency of WBAN resource scheduling. A possible relaxed coloring method is also proposed to skip this tradeoff limitation. Based on the MAC design from chapter 3, solutions for complex priority control of WBAN QoS is further suggested in chapter 4. Finally, chapter 5 summarizes concluding remarks in this WBAN research.

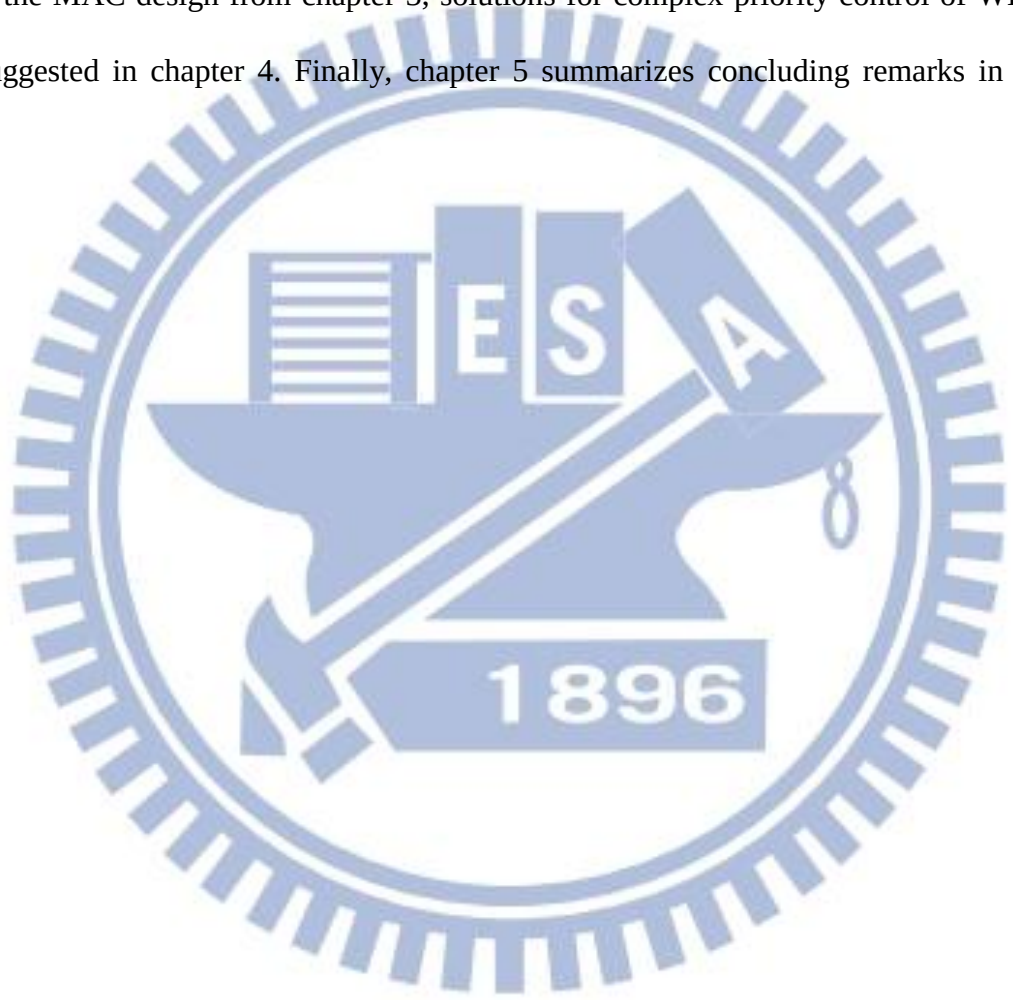

# Chapter 2

# Analysis of multiuser interference

The reason of power consumption may comes from many reasons including overhearing, idle listening, collision, control message, which are identified in [14]. However, for WBAN, collision is the major source of power waste due to its imbalanced network structure. A WBAN consists of a central processing node (CPN) and several wireless sensor nodes (WSNs), which is illustrated in **Fig.** 2-1(a). For the general WBAN scenario, vital signal collection, the major traffic loading comes from the uplink vital signals (**Fig.** 2-1(b)), which implies that WSN is the major transmitter and CPN is the major transmitter. Thus, for WSN, collision is the major source of power consumption. For CPN, overhearing and idle listening are the major sources. The energy spent on control messages can be ignored by assuming that data volume is much larger than the control message. However, the importance of low power CPN is lower than WSN for the reason that CPN, which will most likely be embedded in smart phone or equipments with plug-in power, usually has larger batter than WSN. As a result, how to solve the collision problem of WSN becomes the major issue of low power WBAN.

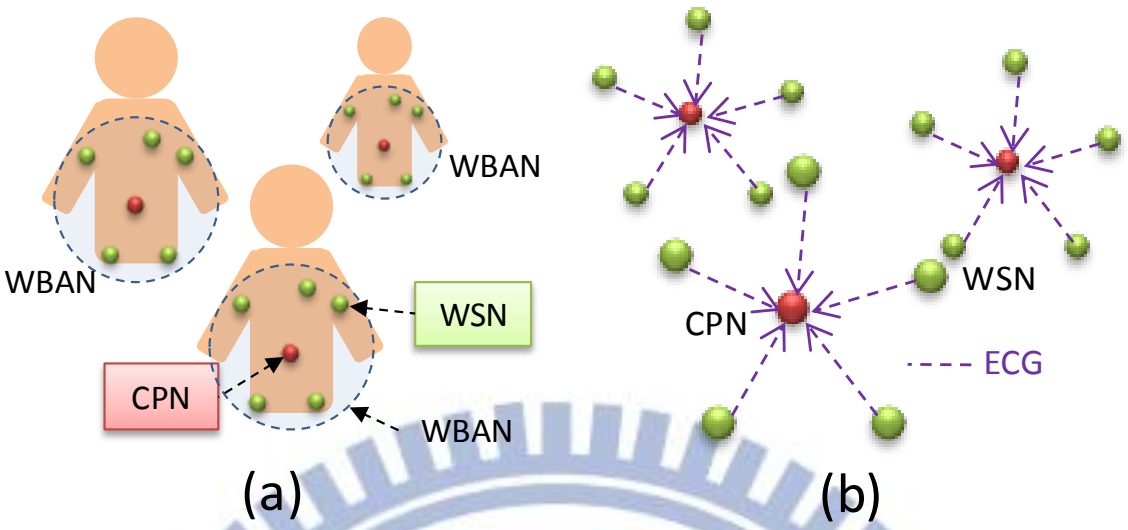


Fig. 2-1 Wireless body area networks (WBAN)
(a) Topology of WBAN (b) Traffic load of WBAN

Similar analytic model for the inter piconet interference of Bluetooth on 2.4GHz unlicensed-band has been studied by [15, 16]. However, for WBAN, WMTS bands [17], which located at 608-614 MHz, 1395-1400 MHz, and 1427-1432 MHz are suggested. These 5 or 6 MHz narrow bands do not allow the frequency hopping of Bluetooth that hops across 80MHz. Thus, [15, 16] cannot be directly used for WBAN analysis.

In this chapter, a time slotted based analytical model is developed to observe the impact of inter WBAN interference of WSN in narrow band. Moreover, this model considers the physical transmission rate and the application data rate, which is expected to provide more realistic mode for WBAN analysis.

## 2.1 WBAN Performance Model of Beacon and Slotted CSMA/CA Modes

To evaluate the performance impact from the inter WBAN collision, two classic medium access methods, Beacon and carrier sense multiple access and collision avoidance (CSMA/CA), are chosen. The tradeoffs between adopting the deterministic (Beacon) and non-deterministic (CSMA/CA) scheduling are expected to be observed through the modeling of the throughput and the power consumption of these two modes. Beacon and CSMA/CA modes have different approaches to handle the WBAN collisions. For Beacon mode, the transmission time of different nodes in the same network are interleaved to avoid the intra network collision (IANC) by using the Beacon message. However, without knowing the transmission schedule of neighbor WBANs, inter WBAN collision (IRNC) cannot be avoided. Different from Beacon mode, CSMA/CA can avoid IANC and IRNC by using detection-backoff-transmission procedure. If a node senses a busy channel, it performs the backoff-detection procedure until an idle channel is available and thus collisions could be avoided. However, the waste of transmission opportunity due to the random backoff might be the potential problem that limits the throughput.

The power model of WBAN considers a fully connected network with $G$ simple-star WBANs and $N$ WSNs per WBAN. As for the WBAN traffic model, 8kbps ECG traffic is continuously transmitted from each WSN to CPN. The power model of WSN can be formulated by two steps. First, we calculate the energy consumption per packet for Beacon and slotted CSMA/CA modes. Next, by calculating the transmission time per packet, the average power consumption in time can be obtained.

We first define an access period $L$ (slots) to fairly compare the performance of these two modes. In both modes, each node attempts to select one slot to transmit a packet within the access period $L$. For the Beacon mode, one access period equals to one Beacon period. By using the Beacon message, CPN can assign one transmission slot for each WSN within the Beacon period. As for slotted CSMA/CA, one access period equals to one contention period. Each WSN will contend for one slot within the contention period of $L$ slots.

Slotted CSMA-CA might need more than one attempts and backoff mechanisms to avoid collision. Each node repeatedly detects channel until the idle channel exists. If the channel is busy, the node backoffs to the next contention period. In this scenario, the energy spent for one packet, $J_{CS}$, is expressed as:

$$J_{CS} = J_{PKT} + J_{CS\_cost} \cdot ATTEMPs_{CS} \tag{2-1}$$

where $J_{PKT}$ is the energy spent on packet transmission. $J_{CS\_cost}$ is the extra energy cost for the channel detection. $ATTEMPs_{CS}$ is the expectation number of contentions before a successful transmission in CSMA/CA. $ATTEMPs_{CS}$ relates to the probability of intra and inter network collisions, $P_{IANC}$ and $P_{IRNC}$ respectively, are expressed as:

$$\begin{aligned} ATTEMPs_{CS} &= \sum_{i=1}^{\infty} i\left(1-P_{IRNC}-P_{IANC}\right)\left(P_{IRNC}+P_{IANC}\right)^{i-1} \\ &= \frac{1}{\left(1-P_{IRNC}-P_{IANC}\right)} = \frac{1}{\left(1-\frac{GN-1}{L}\right)}, 1 \le G \end{aligned} \tag{2-2}$$

where $i$ is the number of attempts. The attempt is repeated until the idle channel exists. The probability of intra network collision, $P_{IANC}$, equals to $1-\left(1-\frac{1}{L}\right)^{N-1}$ by assuming each node uniformly competes with the rest $N-1$ nodes in the same WBAN during the period of $L$. $P_{IANC}$ can be further approximated as $\frac{N-1}{L}$ when $L \gg 1$. For the same reason, $P_{IRNC}$ equals to $1-\left(1-\frac{1}{L}\right)^{(G-1)N}$ and is approximated to $\frac{(G-1)N}{L}$ as $L \gg 1$.

Different from slotted CSMA/CA, the Beacon mode resolves the intra network collision (IANC) by allocating separated time slots for different WSNs. In this case, the cost in the Beacon mode, $J_{BCN\_cost}$, is the listening cost. We assume the Beacon uniformly assigns the slots for each WSN within Beacon period. Collision happens only when two or more nodes from different networks are assigned to the same slot. $P_{IRNC}$ in the Beacon mode is the same as that in CSMA/CA and equals to $\frac{(G-1)N}{L}$. The energy consumption per packet under the Beacon mode $J_{BCN}$ can be expressed as:

$$\begin{aligned} J_{BCN} &= (J_{PKT} + J_{BCN\_cost}) \cdot ATTEMPs_{BCN} \\ &= (J_{PKT} + J_{BCN\_cost}) \sum_{i=1}^{\infty} i\left(1-P_{IRNC}\right) P_{IRNC}^{\,i-1} \\ &= (J_{PKT} + J_{BCN\_cost}) \frac{1}{\left(1-\frac{(G-1)N}{L}\right)}, 1 \le G, N. \end{aligned} \quad \text{(2-3)}$$

Next, we want to relate the $J_{BCN}$ and $J_{CS}$ with the throughput of WSN. We assume all packets have the same fixed size. Thus the throughput can be defined as the packets successfully transmitted per slot time. For instance, in Beacon mode, $ATTEMPs_{BCN}$ implies the number of transmission attempts per packet. Thus, the throughput of WSN in the Beacon mode can be expressed as:

$$Tp_{BCN} = \frac{1}{L \cdot ATTEMPs_{BCN}} = \frac{1}{L\dfrac{1}{\left(1-\dfrac{(G-1)N}{L}\right)}}$$
$$L = \frac{1 \pm \sqrt{1-4Tp_{BCN}(G-1)N}}{2Tp_{BCN}} \qquad (2\text{-}4)$$
$$\frac{1}{4} \geq Tp_{BCN}(G-1)N$$

Equation (2-4) shows the tradeoff between throughput $Tp_{BCN}$ and $(G-1)N$. As shown, if there is a minimum throughput requirement, the maximum number of $G$ implying the number of WBAN users is limited. We found that $L$ has two possible solutions. The throughput in (2-4) is supposed to be higher for small $L$, which means WSN attempts to transmit more often. However, the collision also increases with the increase of the transmission rate. This can be proved from $P_{IRNC}$ in (2-2) with small $L$. Collision decreases the number of successful transmission and makes the throughput lower than expected. From (2-3), larger $L$ has smaller energy consumption. This implies that for given throughput, large $L$ is a better choice than small $L$ because large $L$ can save more energy and reduce the collision rate. With large $L$, $J_{BCN}$ can be rewritten as:

$$J_{BCN} = (J_{PKT} + J_{BCN\_cost}) \cdot \left(\frac{1+\sqrt{1-4Tp_{BCN}(G-1)N}}{1+\sqrt{1-4Tp_{BCN}(G-1)N}-2Tp_{BCN}(G-1)N}\right) \qquad (2\text{-}5)$$

From similar derivations, $J_{CS}$ can also be rewritten as:

$$J_{CS} = J_{PKT} + J_{BCN\_cost}$$
$$\cdot\left(\frac{1+\sqrt{1-4Tp_{CS}(GN-1)}}{1+\sqrt{1-4Tp_{CS}(GN-1)}-2Tp_{CS}(GN-1)}\right)$$
$$Tp_{CS} = \frac{1}{L\left(1-\frac{GN-1}{L}\right)} \qquad (2\text{-}6)$$
$$L = \frac{1+\sqrt{1-4Tp_{CS}(GN-1)}}{2Tp_{CS}}$$
$$\frac{1}{4} \geq Tp_{CS}(GN-1)$$

In the second step, the average power consumption can also be computed by dividing the energy per packet by the transmission time per packet. We assume that the energy only consumed when WSN in TX and RX periods in both modes. During the OFF period, WSN goes to sleep and consumes no power. The power consumption in TX and RX modes is denoted as $W_{ON}$. Thus, the average power of WSN in Beacon mode, $\overline{W}_{BCN}$, is expressed as:

$$\overline{W}_{BCN} = \frac{J_{BCN}}{L \cdot ATTEMPs_{BCN} \cdot Time\_per\_slot}$$
$$= \frac{(J_{PKT} + J_{BCN\_cost}) \cdot ATTEMPs_{BCN}}{L \cdot ATTEMPs_{BCN} \cdot \frac{B_{PKT}}{R_{PHY}}} = \frac{\left(W_{ON} \cdot \frac{B_{PKT}}{R_{PHY}} + W_{ON} \frac{B_{BCN\_cost}}{R_{PHY}}\right)}{L\frac{B_{PKT}}{R_{PHY}}} \qquad (2\text{-}7)$$
$$= W_{ON} \frac{(B_{PKT} + B_{BCN\_cost})}{B_{PKT}} \frac{2\frac{Tp_{bps}}{R_{PHY}}}{1+\sqrt{1-4\frac{Tp_{bps}}{R_{PHY}}(G-1)N}}$$

Where $Tp_{bps}$ (bits/s) is the throughput. $B_{PKT}$ (bits) and $B_{BCN\_cost}$ are the size of data and Beacon packets respectively. $R_{PHY}$ (bits/s) is the minimum transmission rate of physical layer that allows a packet to be transmitted per slot. Following similar steps, $\overline{W}_{CS}$ can be expressed as:

$$\overline{W}_{CS} = W_{ON}\left(\frac{(B_{PKT}+B_{CS\_cost})}{B_{PKT}}\frac{2\frac{Tp_{bps}}{R_{PHY}}}{1+\sqrt{1-4\frac{Tp_{bps}}{R_{PHY}}(GN-1)}} - (GN-1)\left(\frac{2\frac{Tp_{bps}}{R_{PHY}}}{1+\sqrt{1-4\frac{Tp_{bps}}{R_{PHY}}(GN-1)}}\right)^2\right) \quad (2\text{-}8)$$

## 2.2 Analysis and Hybrid Mode

### 2.2.A Power consumption of WBAN

We found that both Beacon and slotted CSMA/CA modes have their own advantage. In **Fig.** 2-2, $N$ is fixed to evaluate the power consumption of WSN with various number of WBAN groups. CSMA/CA mode has lower power consumption than Beacon mode (**Fig.** 2-2) because CSMA/CA adopts the channel detection to avoid collision. The cost of channel detection is lower than the packet collision because the detection will not listen to the channel for whole time of packet receiving. However, with given throughput requirement, CSMA/CA supports less number of WBAN groups treated as overall WBAN user capacity than Beacon mode (**Fig.** 2-3). The body signals monitoring may fail or stop for the insufficient throughput of WSN when the number of user is higher than the limit. Although CSMA/CA has the lowest power consumption, it might fail to meet high user

capacity criterion. To provide both high user capacity and low power WBAN, a new access method should be developed.

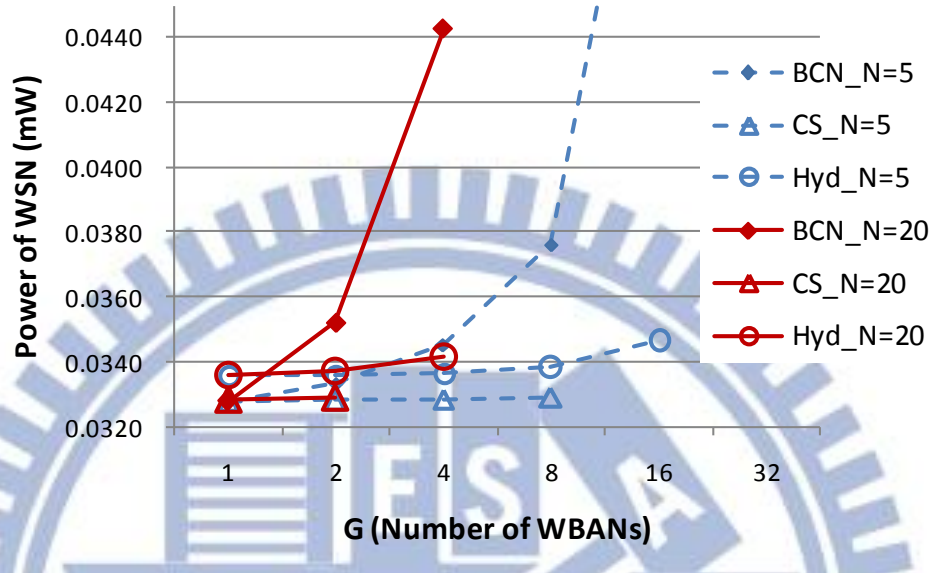


Fig. 2-2 Power consumption of beacon, slotted CSMA/CA, and Hybrid modes.
$W_{ON} = 10mW, Tp_{bps} = 8kbps, B_{BCN/CS\_cost} = 0.2kb, R_{PHY} = 2.5Mbps.$

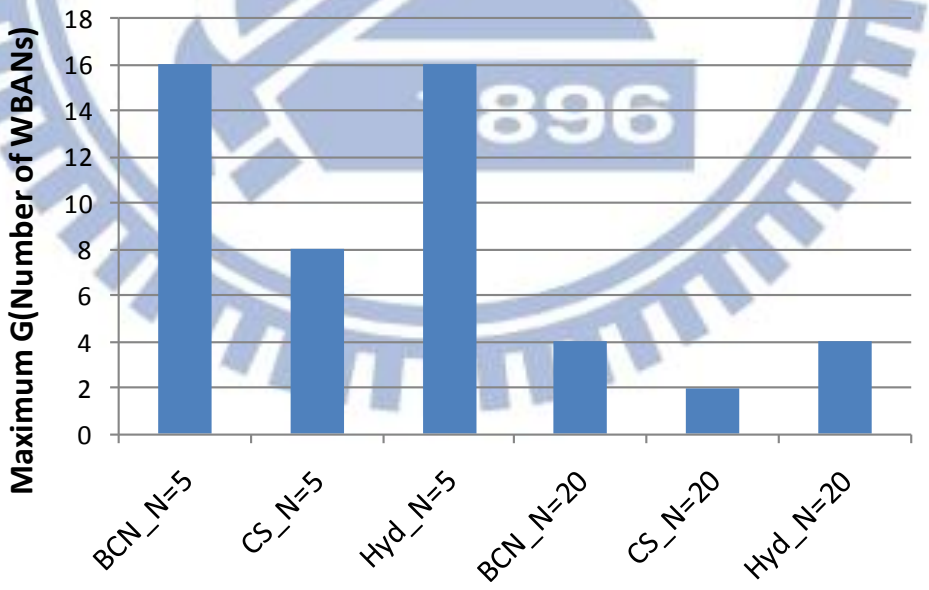


Fig. 2-3 Maximum $G$ (Number of WBANs)
$B_{PKT} = 8kb, Tp_{bps} = 8kbps, R_{PHY} = 2.5Mbps.$

### 2.2.B Hybrid access mode

The proposed Hybrid mode adopting both Beacon and channel detection achieves high user capacity and low power. In the Hybrid mode, Beacon is used to solve the IANC and channel detection is used to handle the IRNC. The Beacon assigns non-overlapped sub contention periods for all WSNs within the Beacon period, which is illustrated in **Fig.** 2-4. This solves the collision from the intra network. For solving IRNC, WSN can perform the channel detection within its own sub contention period to avoid the collision. From **Fig.** 2-2 and 2-3, Hybrid mode has at least 63.4% power consumption of Beacon mode in multi-WBAN scenarios and double user capacity of CSMA/CA mode. Although Hybrid mode costs more power than CSMA/CA because it adopts both Beacon and channel detection, Hybrid mode is still a better access method than CSMA/CA when the required user capacity is high.

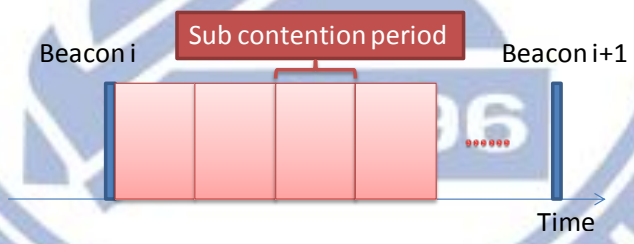


Fig. 2-4 Hybrid access mode

## 2.3 Summary

In this chapter, we have provided an analytical model to analyze the power consumption and capacity limits of different medium access control schemes in mobile WBAN. Results show that neither the Beacon-based nor detection-based access scheme can effectively support both the low power consumption and high capacity (in terms of WSN nodes) simultaneously. A hybrid mode

proposed in this chapter can provide higher capacity while the power consumption is still well managed. This implies a mixed method may be a better solution for WBAN MAC.

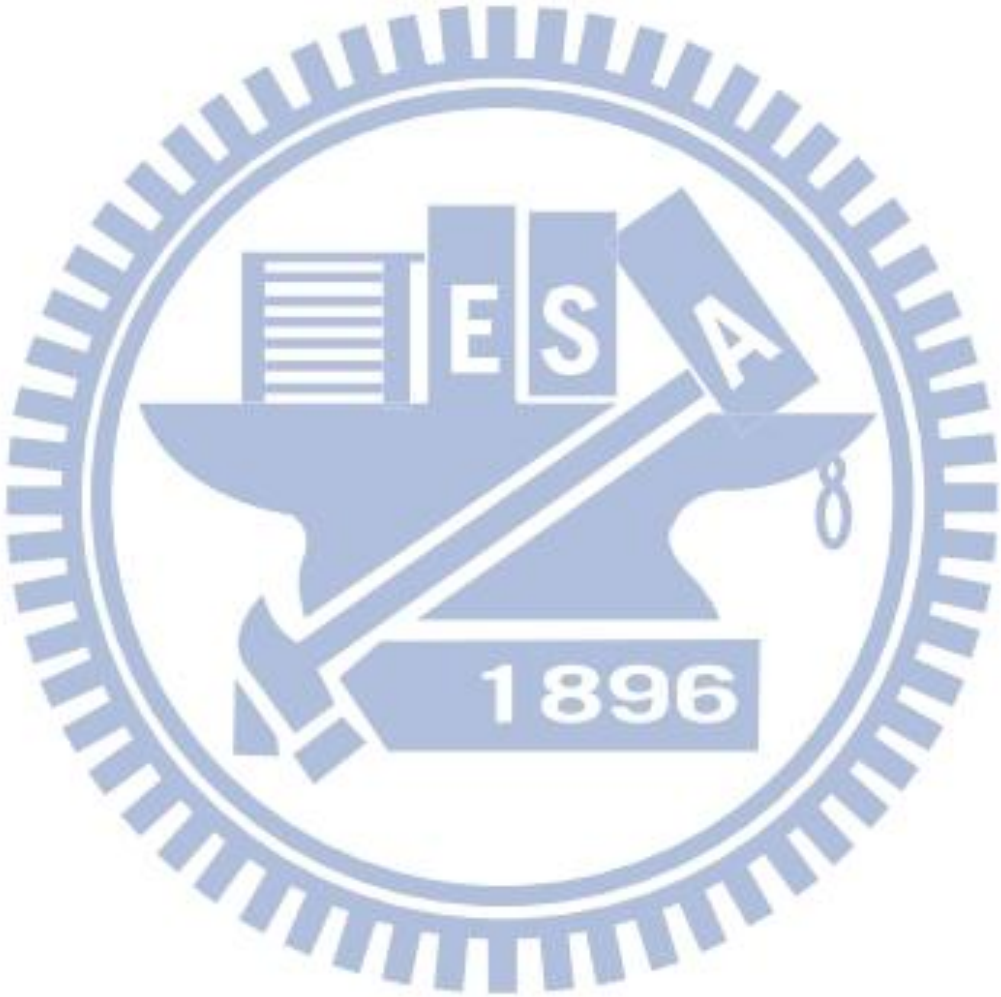

# Chapter 3

# Distributed multiuser resource scheduling

However, unlike a sensor network focused on static or low mobility scenarios [3], a WBAN has a higher moving speed and more frequent topology changes due to user movement [2]. The moving topology of multiple WBANs is similar to that of mobile ad hoc networks (MANETs) [4], but with group-based rather than node-based movement. The "high mobility" and "group-based movement" make the WBAN neither equivalent to a sensor network nor to a MANET. A WBAN thus has a high chance of encountering other WBANs, which creates new issues of inter-WBAN scheduling (IWS). Corresponding discussions [16, 18-21] have just been opened and comprehensive studies are still required.

Distributed interference-avoidance scheduling of wireless networks can be modeled by the notion of distributed graph coloring, which is commonly adopted in sensor networks or MANET [9, 22, 23]. Network topology is modeled as a graph $G=(V,E)$. The vertices $V$ of $G$ represent the wireless nodes; the edges $E$ of $G$ represent radio resource conflicts between mutually-interfering node pairs; the color set $C$ in a coloring of $G$ represents the set of distinct resource units (can be time slots, frequency bands, or code sequences). A complete vertex k-coloring of a graph $G$ is a mapping $V(G)\rightarrow C$, where $|C|=k$, such that adjacent vertices receive distinct colors. Thus, interference between wireless nodes can be avoided by mapping different colors (resource units) to adjacent vertices (mutually-interfering nodes). A standard message-passing model is adopted in this study. To negotiate the color mapping between vertices, they can have a two-way message exchange

with its adjacent vertices. We assume the system is fully synchronous. In other words, all vertices start their coloring algorithms at the same time and execute each step of the algorithm simultaneously. Other terminologies in graph theory refer to [24]. The chromatic number $\chi(G)$ is defined as the minimum $k$ used to completely color graph $G$; $N(v)$ is defined as the set of adjacent vertices of vertex $v$; the maximum degree $\Delta(G)$ is defined as the maximum $d(v)$ and $v \in V(G)$, where vertex degree $d(v) = |N(v)|$.

Two basic requirements of IWS are: (i) fast convergence and (ii) high channel utilization. In the case of a WBAN user walking on a sidewalk, network topology changes frequently when the user keeps encountering other WBAN users. Therefore, a quick IWS that rapidly detects and responds to every topology change is expected, which could adopt the quick $1+\Delta(G)$ coloring for MANET [25]. Also, IEEE 802.15 TG6, the standard task group of WBAN, requires that the WBAN protocol should support at least the sensor density: 60 sensors in a $6^3 m^3$ space [13]. Such dense WBANs create a high probability of mutual interference. It can significantly decrease the number of coexisting WBAN users due to poor channel utilization [19]. Thus, high channel-utilization IWS is also required, which could adopt an optimal spatial-reuse coloring for dense sensor networks [22]. Optimal spatial-reuse implies the maximal number of sensors that access the wireless channel at the same time.

However, references [26-28] show that quick (low time-complexity) coloring and optimal spatial-reuse coloring are trade-offs which cannot be simultaneously achieved with conventional complete coloring. Optimal spatial-reuse coloring uses a minimum number of colors, the chromatic number $\chi(G)$, to color a graph. The fewer colors used, the more there is color-reuse among vertices. It implies more wireless nodes can simultaneously transmit packets using the same resource unit, that is, the system has higher spatial-reuse and channel-utilization. However, completely color a graph by

using $\chi(G)$ colors is known to be NP-complete. The fastest $\chi(G)$-coloring so far still needs time-complexity $O(2^n n^{O(1)})$ [26]. Nevertheless, study [27] indicates that time-complexity can be significantly reduced to $O(\log n)$ if colors are increased to $1+\Delta(G)$ (sacrificing spatial reuse) and distributed coloring techniques are adopted. $1+\Delta(G) \geq \chi(G)$ is known as Brooks' theorem, which is a loose upper bound for $\chi(G)$. A recent work [29] adopts a similar $1+\Delta(G)$ coloring method. It guarantees not only $O(\log n)$ time-complexity but also $O(\log n)$ bit complexity, which is the amount of information exchanged between vertices during coloring. Low-bit-complexity of a coloring algorithm makes it applicable to low-computing-power applications, such as sensor networks. Although [28] further decreases the time complexity from $O(\log n)$ to[2] $\tilde{O}(\sqrt{\log n})$ by applying vertex priority, $1+\Delta(G)$ colors are still required. As a result, neither $\chi(G)$ [26] nor $1+\Delta(G)$-coloring [27, 28] may be directly applied to IWS due to their high time-complexity and low spatial-reuse, respectively.

This chapter proposes Random Incomplete Coloring (RIC) to realize quick and high spatial-reuse IWS. RIC consists of 1) a proposed random-value coloring method and 2) an incomplete-coloring approach. The random-value coloring method is a technique which realizes prioritized vertex coloring [28] (so-called oriented coloring) and will be proven to have a low time-complexity[3] $O\left(e^{W(2\ln n)/2}\right)$, which is even lower than [28] . Besides, for high spatial-reuse coloring, conventional complete coloring using $\chi(G)$ colors is known as the solution for optimal spatial-reuse. Surprisingly, for designs of wireless resource scheduling, this study found that higher spatial-reuse (on average) than that of $\chi(G)$ coloring is possible if partial vertices are allowed to be uncolored

[2] Soft-O: $\tilde{O}(g(n))$ is short for $O(g(n)\log^k g(n))$.

and only $k < \chi(G)$ colors are used. In wireless networks, we observe that uncolored vertices imply wireless nodes with no transmission, which do not interfere each other. Hence, following the nature of wireless communication, there is no conflict between adjacent uncolored vertices (or with the special color: no color). Based on this fact, we can color a subgraph of graph $G$. This subgraph is constructed using vertices, excluding uncolored ones. Clearly, it is possible to use less colors for the subgraph. For convience, we name this kind of coloring "incomplete" coloring. The proposed Random Incomplete Coloring (RIC) will be implemented as an inter WBAN scheduling protocol with a TDMA framing structure, a common structure used in sensor or body area networks [2], to test its convergence speed and spatial reuse in various mobile WBAN scenarios.

The rest of this chapter is organized as follows: section 3.1 introduces the details of related works and the problem formulation. Section 3.2 reveals the proposed RIC algorithm. The corresponding analytical models of RIC are provided in section 3.3. Section 3.4 presents the simulation settings and results. Section 3.5 concludes this chapter.

## 3.1 Related Works and the WBAN System Model

### 3.1.A Oriented and Non-oriented Coloring

Oriented vertex coloring [28] is a distributed coloring technique that utilizes predefined edge orientation (vertex priority) to improve the coloring speed of (non-oriented) random vertex coloring [27] from $O(\log n)$ to $\tilde{O}(\sqrt{\log n})$. Here we refer to [27] as non-oriented vertex coloring to distinguish [28] from [27]. The major difference between oriented and non-oriented coloring is the

[3] $W(x)$ is the Lambert W function [18]. $W(x)$ is solved by inverting the equation,

manner of solving color conflicts, as shown in **Fig.** 3-2 Step 3. For non-oriented coloring, when color conflict $c_u = c_v$ happens to vertices pair $(u,v)$, both vertices give up that color and re-choose new colors for the color contention in the next coloring round. In contrast, oriented coloring tries to force the vertex that has a higher priority (having an outward edge orientation) to win the color. Although an oriented conflict-path may exist ($u \to v \to w$, $c_u = c_v = c_w$) and only the vertex $u$ at the start of the path can win the color (no vertex has a higher priority than $u$ has), oriented coloring generates at least one winner for each path in each round (an exception, deadlock circle, will be mentioned later). This is the reason why oriented coloring speeds up coloring.

Given $G = (V,E)$; $u,v \in V(G)$; $C_u(r)$ is the set of available colors of $u$ in coloring round $r$; The initial size of the available color set is $|C_u(0)| = k = 1 + \Delta$; every edge $(u,v) \in E(G)$ has a predefined orientation. For each coloring cycle:

While $u$ is uncolored,

1. $u$ chooses a color $c_u$ from $C_u(r)$.
2. $u$ broadcasts a coloring message with $c_u$ to adjacent vertices in $N(u)$.
3. If $u$ receives coloring messages from $v \in N(u)$ and
   *if* (**non-oriented coloring** )
   $u$ is colored by $c_u$ only when $c_u \neq c_v$.
   *elseif* (**oriented coloring** )
   $u$ is colored by $c_u$ when (i) $c_u \neq c_v$ or (ii) $c_u = c_v$ with edge orientation $u \to v$.
   *endif*
4. if $u$ wins the color, it broadcasts the color taken notification.
5. $u$ removes the colors taken by $N(u)$ from $C_u(r+1)$.

Fig. 3-2 Oriented and non-oriented colorings (Pri-arts)

---

$z = W(z)\exp[W(z)]$, for any complex number $z$.

However, to realize the oriented coloring for IWS, two particular issues need to be considered: (i) fairness and (ii) oriented conflict-circle (deadlock circle). First, oriented coloring assumes the priorities of vertices are pre-defined, which is not practical for the dynamic topology of a WBAN. How to dynamically and fairly decide the priority of a WBAN should be further addressed. The second issue is the oriented conflict-circle (deadlock circle) problem. An oriented conflict-circle is defined as a circle graph with one-way orientation and vertices in the circle contending for the same color (e.g. $u \to v \to w \to u, c_u = c_v = c_w$). There is no vertex in that circle that can be colored because there is always another adjacent vertex with a higher priority. Thus, the coloring cannot be completed unless vertices try to contend using different colors in subsequent rounds. To solve these two problems, a method that implements oriented coloring, random value coloring, is proposed. Moreover, we will show that this method can further decrease the time complexity from $\tilde{O}(\sqrt{\log n})$ [28] to $O\left(e^{W(2\ln n)/2}\right)$.

Aside from the above implementation issues, conventional complete colorings [26-28], including oriented coloring [28], have an optimum spatial reuse bounded by $\chi(G)$. However, for designs of wireless resource scheduling, spatial reuse can be further improved if the coloring rule is relaxed. The relaxed coloring approach, referred to as incomplete coloring, will be introduced in the next section.

### 3.1.B CPN-based IWS

A CPN-based IWS will be adopted in this study due to the imbalanced CPN/WSN architecture of a simple star (**Fig.** 3-1). In a single WBAN, the CPN plays the role of the master and the WSNs are the slaves. The CPN manages the join, leave, and functional-control of the WSNs. In contrast, WSNs

are passive devices, which are designed to retrieve specific vital signals such as blood pressure or electrocardiograms (ECG) and forwarding them to the CPN. Besides, a CPN is most likely to be embedded in personal devices such as cellular phones or PDAs with larger and rechargeable batteries. In contrast, a WSN is expected to be light weight (small battery) and even non-rechargeable for certain implantable applications. These two unbalanced features suggest shifting power-consuming network controls from WSNs to the CPN. Thus, a CPN-based two-step IWS, which is illustrated in **Fig.** 3-3, is assumed in this study. The CPN first negotiates the WBAN resources with other CPNs that are in the mutually-interfering-range. The CPN then assigns reserved resources to its WSNs. As a result, the WSN wakes up only when (1) receiving beacon messages carrying the pre-regularized transmission schedule from the associated CPN and (2) transmitting vital signals following the schedule to that CPN.

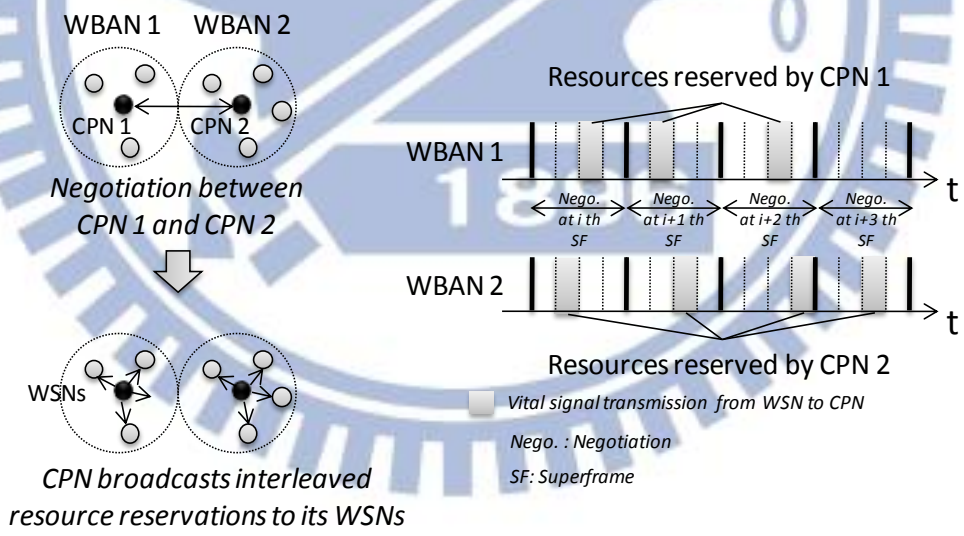


Fig. 3-3 CPN-based inter-WBAN scheduling (IWS)

The CPN-based IWS can now be modeled as a unit-disk graph coloring problem. A 2-dimensional randomly constructed graph (in short, random graph) $G=(V,E)$ is generated to model the WBAN network. $V(G)$ represents the set of CPNs; $E(G)$ represents the set of conflict links between

CPNs. The first step in generating the graph is to randomly deploy $n=|V(G)|$ vertices in a field to simulate the random positions[4] of WBAN users. Consequently, edges are added to connect vertices if the distance between CPNs is equal to or less than the mutually-interfering-range between WBANs (the radius of the unit-disk). In this sense, the graph of CPN-based IWS is similar to that of MANET scheduling. However, they have different resource scheduling strategies. In MANET, each vertex represents a wireless node. MANET focuses on efficient inter-node communication and routing. Hence, "edge" coloring, which models the scheduling of "node-to-node communications", can be adopted. In contrast, in CPN-based IWS, each vertex represents a sensor group (WBAN). CPN-based IWS tries to resolve the interference between sensor groups belonging to different users. Therefore, "vertex" coloring, which models the scheduling of active "CPN-based sensor groups", is appropriate. As a result, for CPN-based IWS, a k-coloring of the random graph is labeled $V(G)\rightarrow C$, where $|C|=k$, such that adjacent vertices receive distinct colors. The labels are colors, which are mapped to different resource units for associated data transmissions (WSNs to the CPN). Only k resource mappings can be decided when a k-coloring algorithm is excuted once. We assume that every WSN always has data to be transmitted to the CPN. Hence, the coloring is periodically performed to map wireless resources to all these data transmissions. The target of this study is to devise a coloring method that simultaneously satisfies two IWS requirements: (i) low time-complexity and (ii) high spatial reuse.

4 In some cases, waiting lines for example, user positions follow certain rules instead of random deployments, which yield special graphs such as lines or grids. Although these graphs might reflect more real scenarios in our life than the random graph does, they need more complicated analysis skills due to their restrictions of graph formation. Therefore, to make the discussion of the proposed RIC more intuitive, this study focuses on the performance analysis of the random graph.

## 3.2 Random Incomplete Coloring

The proposed random incomplete coloring (RIC) has two major components: (i) a proposed random-value coloring method and (ii) a proposed incomplete coloring approach. The random value coloring is a low time-complexity coloring method, which is designed for quick IWS. On the other hand, incomplete coloring is a high spatial-reuse coloring approach, which modifies the conventional coloring rule to explore the potential high spatial reuse when $k < \chi(G)$.

### 3.2.A Random Value Coloring

Random value coloring is a method that realizes oriented coloring. It overcomes two major problems of oriented coloring [28] : fairness and oriented conflict-circle (deadlock circle), as outlined in section 3.1.A. The method of random value coloring is to adopt a random value comparison to generate instant priority differences between all adjacent vertices, as illustrated in **Fig.** 3-4 (except step 6 for the incomplete coloring).

***Random Incomplete Coloring:***

Given $G=(V,E)$, $u \in V$; $C_u(r)$ is the set of available colors of $u$ in coloring round $r$. The initial size of the available color set is $|C_u(0)|=k$. For each coloring cycle:

While $u$ is uncolored,

1. $u$ chooses a color $c_u$ from $C_u(r)$ with a random value, $\Re_u$.
2. $u$ broadcasts its RVC message including $c_u$ and $\Re_u$ to $N(u)$.
3. If $u$ receives RVC messages from $v \in N(u)$ with $\Re_v \geq \Re_u$ and $c_v = c_u$, $u$ remains uncolored. Otherwise, $u$ is colored by $c_u$. (***Random value coloring***)
4. if $u$ wins the color, it broadcasts the color taken notification.
5. $u$ removes the colors taken by $N(u)$ from $C_u(r+1)$.
6. If $|C_u(r+1)|=0$, $u$ becomes uncolored. (***Incomplete coloring***)

Fig. 3-4 Random incomplete coloring

In **Fig.** 3-4, the fairness of random value coloring can be supported if the random values $\Re$ from different vertices are generated with an identical uniform distribution[5]. Due to the symmetry between vertices, it is obvious that the probability that a vertex generates the maximum random value (wins the color) among $(n-1)$ competitors is $1/n$, where "competitors" means adjacent vertices contending for the same color. Thus, each vertex has equal radio resource sharing with its adjacent vertices. Besides, the way that random value coloring avoids an oriented conflict-circle can easily be observed, since it is not possible to have the ordering of the random values of vertices in a circle with

[5] $f(x)=1/(b-a), a \leq x \leq b$, otherwise $f(x)=0$.

a one way orientation $\Re_{v1} > \Re_{v2} > \cdots > \Re_{vn} > \Re_{v1}$. The fairness and deadlock-circle-free properties of the proposed method makes oriented coloring possible to realize for quick IWS.

### 3.2.B Incomplete Coloring

Incomplete coloring improves spatial reuse by greedily coloring a graph with $k < \chi(G)$. Normally it is not possible to completely color a graph using $k < \chi(G)$ colors because color conflict is unavoidable and cannot be resolved[6]. Thus, incomplete coloring allows uncolored vertices to avoid conflict when vertices run out of $k$ colors, as illustrated at step 6 of **Fig.** 3-4. Note that when applying incomplete coloring to IWS, the uncolored node means a CPN reserves no resource in that coloring. The WBAN of this CPN becomes temporarily inactive and generates no interference with its neighbor WBANs. The example in **Fig.** 3-5 demonstrates how incomplete coloring improves spatial reuse (on average).

[6] Assume $k < \chi(G)$ and $G$ can be completely colored by $k$ colors (adjacent vertices receive distinct colors). However, $\chi(G)$ is defined as the minimum colors to completely color $G$ and thus $k \geq \chi(G)$ contradicts $k < \chi(G)$. As a result, there must be adjacent vertices that receive the same color.

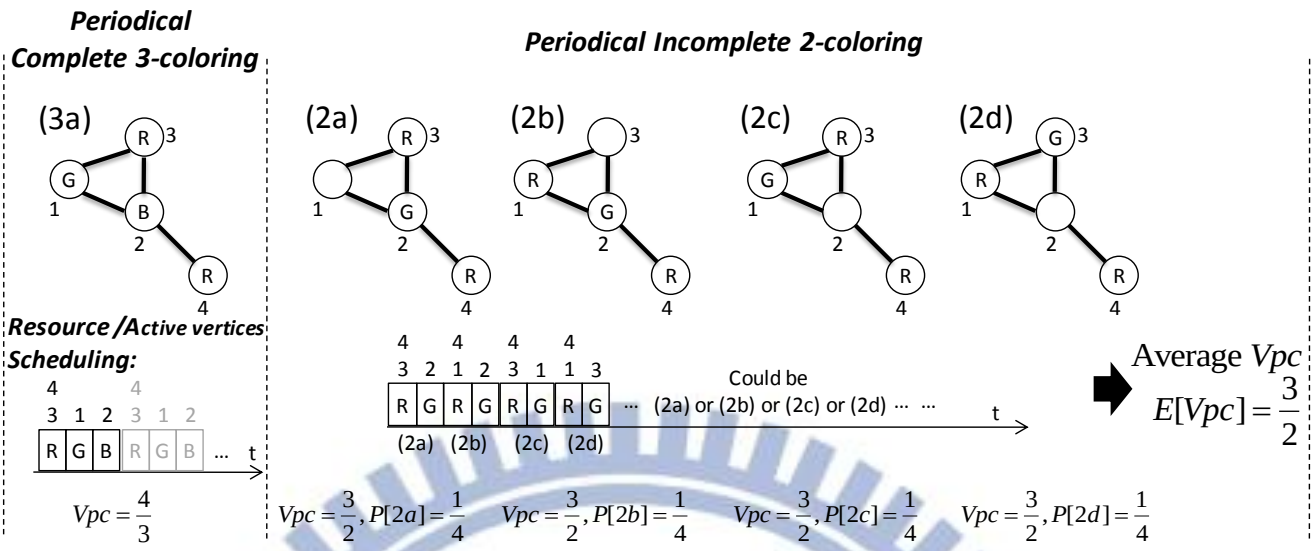


Fig. 3-5 Random incomplete coloring

**Definition 3.1** Vertices-per-color (*Vpc*), which is defined as the average number of vertices colored by each color, is used to evaluate the average spatial reuse (color reuse) of periodical coloring. Higher *Vpc* implies more wireless nodes can simultaneously transmit packets using the same resource unit (color), that is, the system has higher spatial-reuse on average.

**Definition 3.2** A coloring round is defined as the execution of all steps in the while loop of the coloring algorithm (e.g. steps 1 to 6 in **Fig.** 3-4). A coloring cycle is defined as the execution of all the coloring rounds required to leave the while loop, that is, the end of the algorithm.

Graph $G$ with 4 vertices in **Fig.** 5 can be completely colored by $\chi(G)=3$ colors (case (3a)), written $\varphi_3$. Thus, $Vpc(\varphi_3)=4/3$. On the other hand, if two colors are used for incomplete coloring ($k=2$), written $\varphi'_2$, there are four possible results at the end of the coloring cycle: 2a to 2d. Because 2a to 2d all have 3 vertices colored by 2 colors, 2a to 2d have identical $Vpc=3/2$. The probability that each case happens depends on the color contention scheme. Assume a random value

coloring method is adopted. Because cases 2a to 2d are symmetric and vertices 1 to 4 have equal priority in the contention, each case has an identical $1/4$ probability of showing up. As a result, when the incomplete coloring with $k=2$, $\varphi'_2$, is iteratively performed, $E\left[Vpc\left(\phi'_2\right)\right]=3/2$ for each coloring cycle. There is an increase of 12.5% over $Vpc\left(\varphi_3\right)=4/3$ on average.

Of course, the 3-color complete coloring schedules one more resource than the 2-color incomplete coloring in each coloring cycle. In periodical coloring, to schedule the same number of resources, a k-color incomplete coloring ($k<\chi(G)$) needs $\chi(G)/k$ times more coloring cycles than that of a $\chi(G)$-color complete coloring, which increases the exchange of coloring messages required for periodical coloring. This could affect the collision probability of coloring messages in a practical IWS implementation. The tradeoffs between spatial reuse and affordable coloring-message exchanges will be closely analyzed in section 3.4.

## 3.3 Analytical Model of Random Value and Incomplete Coloring

### 3.3.A Upper Bound of the time and bit complexity of RIC

With the proposed random value coloring method, the time complexity of RIC can be further decreased from $\tilde{O}(\sqrt{\log n})$ [28] to $O\left(e^{W(2\ln n)/2}\right)$, where $W(x)$ is the Lambert W function [30]. The time-complexity (upper bound) of RIC to color a graph with a constant-degree $\Delta$ is calculated. This could be used to observe the time complexity of the 2-D topology model. Because vertices are randomly deployed in the 2-D model, every vertex should have a similar vertex degree. The accuracy of this constant-degree assumption will be verified in the section 3.4.A.

**Definition 4.1** Oriented conflict-path (OCP) is defined as a path with all edges having a one-way orientation and all vertices in this path contending for the same color.

**Lemma 4.2** A graph having the longest OCP with $l$-length ($l$-vertices) can be colored in at most $l$ rounds.

This lemma is proved by [28], which shows that, in each coloring round, at least one vertex can be colored in the OCP. Thus, a graph with an $l$-length OCP can be colored within $l$ rounds.

**Lemma 4.3** The probability that an OCP has length larger than or equal to $i$ in round $r$ of the RIC algorithm is less than or equal to $\left(\left(\frac{1}{k}\right)^{i-1}\cdot\frac{1}{i!}\right)^{r}$.

For the RIC algorithm, an OCP is only generated when the random values of vertices in the path are in descending order, $\Re_{v1}>\Re_{v2}>\Re_{v3}>\cdots$ (Definition 4.1). Therefore, the probability that an OCP has length larger than or equal to $i$ can be expressed as

$$\begin{aligned}
&k\left(\frac{1}{k}\right)^{i}\cdot P\left[\Re_{v1}>\Re_{v2}>\cdots>\Re_{vi}\right]\\
&=k\left(\frac{1}{k}\right)^{i}\cdot\prod_{m=1}^{i}P\left[\Re_{vm}=Max\left\{\Re_{vn},n\in[m,i]\right\}\right]\\
&=k\left(\frac{1}{k}\right)^{i}\cdot\prod_{m=1}^{i}\frac{1}{m}\quad\text{(Due to the symmetry of }\Re_{vm}\text{)}\\
&=k\left(\frac{1}{k}\right)^{i}\cdot\frac{1}{i!}=\left(\frac{1}{k}\right)^{i-1}\cdot\frac{1}{i!}
\end{aligned}\qquad\text{(3-1)}$$

Where $k$ is the number of colors used in the RIC. The length of the OCP can only decrease or stay the same during the coloring. Hence, to make sure the length of an OCP is larger than or equal to

$i$ in round $r$, the length of this OCP should always be larger than or equal to $i$ from round 1 to round $r$. Therefore, the probability that an OCP has length larger than or equal to $i$ in round $r$ is less than or equal to $\left(\left(\frac{1}{k}\right)^{i-1}\cdot\frac{1}{i!}\right)^{r}$.

**Theorem 4.4** Given a graph with $n$ vertices and constant degree $\Delta$, the time complexity of the RIC algorithm for any number of colors is $O\left(e^{W(2\ln n)/2}\right)$ rounds, where $W(x)$ is the Lambert W function.

**Proof:** A two-phase analysis, which is similar to [28, 31], is adopted to calculate the time complexity of the proposed RIC algorithm. Phase I lasts from the first coloring round to $r_\Gamma{}^{th}$, $r_\Gamma = 10e^{W(2\ln n)/2}$ rounds; Phase II lasts from $\left(r_\Gamma+1\right)^{th}$ rounds to the end of the coloring cycle. A graph may contain multiple OCPs during the coloring. At the end of Phase I, we prove that the length of any OCP of the graph will be confined by the length $l_\Gamma = e^{W(2\ln n)/2}$ with a high probability. According to **lemma 4.2**, this graph can be further colored with at most $e^{W(2\ln n)/2}$ coloring rounds in Phase II. Thus, the total coloring rounds can be proved to be $O\left(10e^{W(2\ln n)/2}\right)+O\left(e^{W(2\ln n)/2}\right)=O\left(e^{W(2\ln n)/2}\right)$.

At the end of Phase I, the length of any OCP will be proven to be confined by the length $l_\Gamma = e^{W(2\ln n)/2}$ with a high probability. This can be a dual proof: there is a low probability that at least one OCP of the graph is of length larger than $l_\Gamma$ at the end of Phase I. This probability is denoted as $P[\mathbb{E}]$. The probability of an OCP in such event is denoted as $P\left[l\left(r_\Gamma\right)>l_\Gamma\right]$, where $l\left(r_\Gamma\right)$ is the

length of the OCP in round $r_\Gamma$. Also, in a graph with $n$ vertices, $n\Delta^i$ is the maximum[7] number of OCPs with length $i$. Therefore,

$$\begin{aligned} P[\mathbb{E}] &\le \sum_{i=l_\Gamma+1}^{n} n\Delta^i \cdot P\left[l(r_\Gamma)=i\right] \\ &\le \sum_{i=l_\Gamma+1}^{n} n\Delta^i \cdot P\left[l(r_\Gamma)\ge i\right] \\ &\le \sum_{i=l_\Gamma+1}^{n} n\Delta^i \cdot \left(\left(\frac{1}{k}\right)^{i-1} \cdot \frac{1}{i!}\right)^{r_\Gamma} \quad \text{(Lemma 4.3)} \end{aligned} \tag{3-2}$$

For simplicity in the following calculation, the approximation of the factorial term, $i! \ge e\left(\frac{i}{e}\right)^i$, is applied. Thus $\sum_{i=l_\Gamma+1}^{n} n\Delta^i \cdot \left(\left(\frac{1}{k}\right)^{i-1} \cdot \frac{1}{i!}\right)^{r_\Gamma} \le \sum_{i=l_\Gamma+1}^{n} n\Delta^i \cdot \left(\left(\frac{1}{k}\right)^{i-1} \cdot \frac{1}{e\left(i/e\right)^i}\right)^{r_\Gamma}$. Each term in the summation can be simplified to $n\Delta^i \cdot \left(\frac{k^{10}}{e^{10}}\right)^{l_\Gamma} \left(\frac{e^{10}}{k^{10}}\right)^{i \cdot l_\Gamma} \frac{1}{\left(i^{i \cdot l_\Gamma}\right)^{10}}$, which is less than or equal to $\frac{n}{\left(i^{i \cdot l_\Gamma}\right)^7}$ due to $i^{i \cdot l_\Gamma} > O(1)^{i \cdot l_\Gamma} > O(1)^i > O(1)^{l_\Gamma}$ (recall that $i > l_\Gamma$). Also, $\frac{n}{\left(i^{i \cdot l_\Gamma}\right)^7} \le \frac{n}{\left(l_\Gamma{}^{l_\Gamma{}^2}\right)^7}$ and $l_\Gamma = e^{W(2\ln n)/2}$ lead to $n = l_\Gamma{}^{l_\Gamma{}^2}$ (recall that $z = W(z)\exp[W(z)]$, for any complex number $z$). Therefore, $P[\mathbb{E}] \le \sum_{i=l_\Gamma+1}^{n} \frac{n}{n^7} \le \frac{1}{n^5}$, which approaches 0 as $n \to \infty$. As a result, at the end of Phase I, the lengths of any OCPs confined by $l_\Gamma = e^{W(2\ln n)/2}$ are proved with a high probability. The upper bound of total rounds that the RIC algorithm requires is the summation of the maximum rounds of Phases I and II, $O\left(10e^{W(2\ln n)/2}\right) + O\left(e^{W(2\ln n)/2}\right) = O\left(e^{W(2\ln n)/2}\right)$, Q.E.D.

[7] Because each OCP could start from any of $l_\psi = e^{W(2\ln n)/2}$ vertices. Also, each vertex has $\Delta$ adjacent vertices in the constant $\Delta$ degree graph, so there are $\Delta^i$ possible combinations to generate an OCP with

**Definition 4.5** As is explained in [29], the bit complexity of a distributed algorithm (per channel) is defined as the total number of bits exchanged (per channel) during its execution.

**Theorem 4.6** The bit complexity of the RIC algorithm is $O\left(e^{W(2\ln n)/2}\log n\right)$.

In each coloring round of the RIC algorithm, each vertex exchanges one random number and one color identification with each neighbor on each channel. We assume the random number has finite resolution and hence can be expressed by bits with a constant bit length $C$. Also, the necessary colors for a n-vertices-graph coloring can always be identified by $O\left(\log n\right)$bits. As a result, for the RIC, the number of bits exchanged in a coloring cycle ($O\left(e^{W(2\ln n)/2}\right)$ rounds) is $O\left(e^{W(2\ln n)/2}\log n\right)$.

### 3.3.B Spatial Reuse of Incomplete Coloring

Similar to the time complexity analysis, the $Vpc$ of RIC for a constant degree $\Delta$ graph is calculated. $P_c$ is defined as the probability that a vertex can be colored by RIC. In the constant degree graph, the $P_c$s of all vertices are identical due to the symmetric graph structure. Each $k$ coloring decides a $k$-color vertex-to-color mapping. Thus, $Vpc = n\frac{P_c}{k}$, where $n$ is the number of vertices in the graph. Consequently, to calculate the $Vpc$, all we need to know is the value of $P_c$.

Theorem 4.5 For a graph with constant degree $\Delta$, the probability that each vertex can be colored by the algorithm RIC, written as $P_c$, is satisfied by the equation $P_c = \sum_{i=1}^{k}(-1)^{i-1}\binom{k}{i}\left(1-i\frac{P_c}{k}\right)^{\Delta}$.

---

length $i$.

**Proof:** The idea of the $P_c$ calculation is based on the probability complementary between each vertex and its adjacent vertices. In RIC, the probability that a vertex can be colored is $P_c = \sum_{i=1}^{k} P_{c_i}$, where $P_{c_i}$ represents the probability that the vertex is colored by color $c_i$. If a vertex can be colored, its adjacent vertices must have the color combinations without using $c_1$ or $c_2$ or $\cdots$ or $c_k$, written $P\left[\bigcup_{i=1}^{k} \overline{c_i}\right]$, where $\overline{c_i}$ denotes that adjacent vertices are not colored by $c_i$. Thus, $P_c = \sum_{i=1}^{k} P_{c_i} = P\left[\bigcup_{i=1}^{k} \overline{c_i}\right]$, which can be expressed as:

$$\begin{aligned} P\left[\bigcup_{i=1}^{k} \overline{c_i}\right] &= \sum_{i=1}^{k} P\left[\overline{c_i}\right] - \sum_{i,j:1\le i<j\le k} P\left[\overline{c_i} \cap \overline{c_j}\right] \\ &+ \sum_{i,j,l:1\le i<j<l\le k} P\left[\overline{c_i} \cap \overline{c_j} \cap \overline{c_l}\right] - \cdots + (-1)^{k-1} P\left[\overline{c_1} \cap \cdots \cap \overline{c_k}\right] \\ &= \sum_{i=1}^{k} \left(1 - P_{c_i}\right)^{\Delta} - \sum_{i,j:1\le i<j\le k} \left(1 - P_{c_i} - P_{c_j}\right)^{\Delta} \\ &+ \sum_{i,j,l:1\le i<j<l\le k} \left(1 - P_{c_i} - P_{c_j} - P_{c_l}\right)^{\Delta} - \cdots + (-1)^{k-1} \left(1 - P_{c_1} - \cdots - P_{c_k}\right)^{\Delta} \end{aligned} \tag{3-3}$$

Due to the symmetry of each color in the equation, $P_{c_1} = P_{c_2} = \cdots = P_{c_k} = \frac{P_c}{k}$, thus

$$P_c = \sum_{i=1}^{k} (-1)^{i-1} \binom{k}{i} \left(1 - i\frac{P_c}{k}\right)^{\Delta} \tag{3-4}$$

As a result, $P_c$ can be obtained by solving for the real root of (3-4).

## 3.4 Computer Simulation

A two-stage performance evaluation of RIC is provided in this section. The first stage evaluates the time-complexity and spatial reuse of the RIC. At the second stage, RIC is applied in an IWS with a TDMA framing structure, a common structure used in sensor or body area networks [2]. It tests the convergence speed and channel utilization of IWS in mobile WBAN scenarios. Packet collisions of data packets and coloring messages will be considered in the second stage.

### 3.4.A Performance Evaluation of RIC

2-D random graphs with various vertex densities are used to evaluate the performance of the RIC. Following the system model in Section 3.1, $n$ vertices are randomly deployed in a $10\times10\,m^2$ square. The mutually-interfering-range is set as 2m. $n$ can be 12, 25, 50, 100 to simulate low, middle, high, and extremely high densities. The performance metrics used to evaluate time complexity and spatial reuse of coloring are rounds-per-cycle ($Rpc$) and vertices-per-color ($Vpc$) respectively. $Rpc$ is defined as the total coloring rounds required to finish a coloring cycle.

**Fig.** 6 compares the $Rpc$ of the proposed RIC with INC-only. INC-only is an incomplete coloring combined with non-oriented coloring [27]. Due to the low time-complexity of the RIC, $O\left(e^{W(2\ln n)/2}\right)$, **Fig.** 6 shows that RIC can be finished within five rounds in any number of colors (1~15 colors) and vertex densities (12~100 vertices). In contrast, the coloring rounds of INC-only dramatically increase, especially when the vertex density is high or few colors are used. This huge difference comes from the different strategies of RIC and INC-only in dealing with color conflict. RIC forces each color conflict to generate a winner. On the other hand, for INC-only, vertices in the

conflict pair both give up the conflict color and re-select new colors in the next coloring round, which prolongs the coloring time. The time-complexity of INC-only grows significantly in the few $k$ (reduced color choices) or the high density (increasing competitors) scenarios.

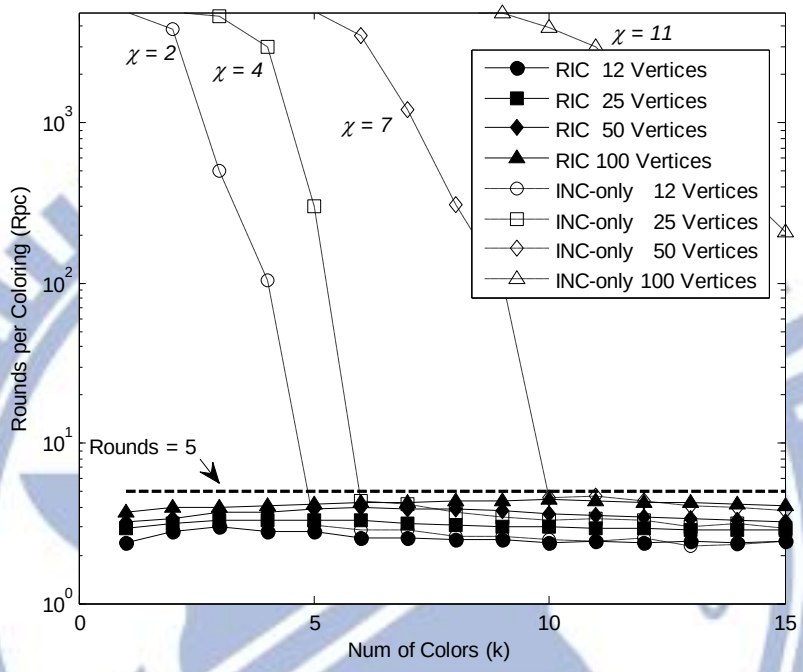


Fig. 3-6 Rounds per coloring cycle ( *Rpc* ) of RIC and INC-only

For the spatial reuse analysis of RIC, **Fig.** 7 compares the analytical model (theorem 4.5 based on the constant-degree graph assumption) with simulation results for RIC in a 2-D random graph. **Fig.** 7 shows that the analytical model can correctly predict the *Vpc* of RIC, which monotonously increases while the number of colors $k$ decreases.

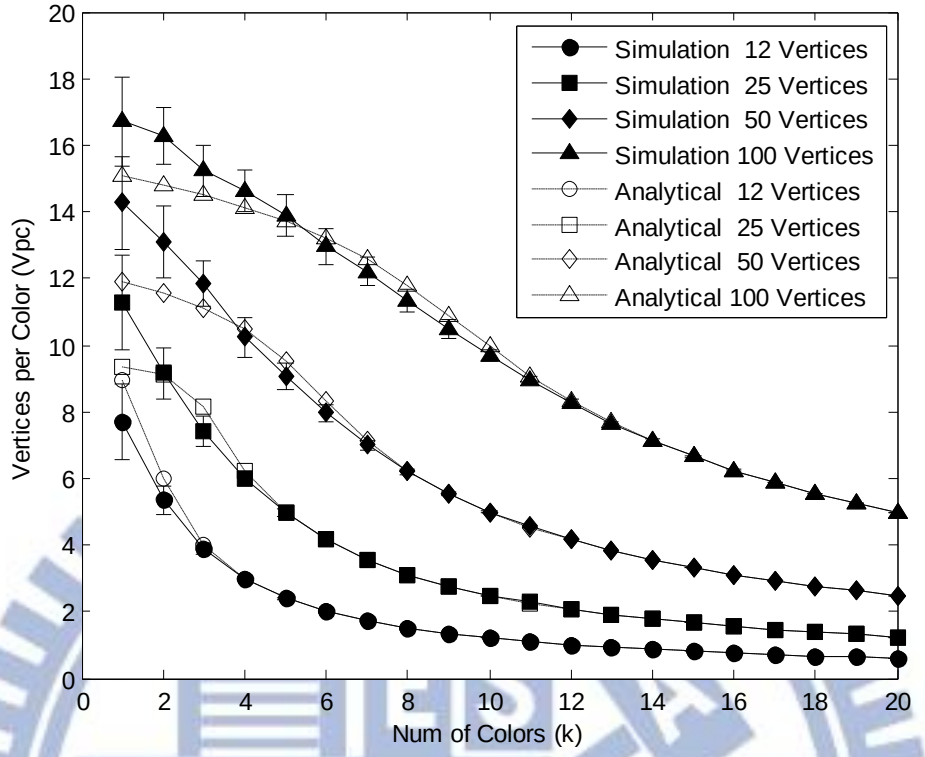


Fig. 3-7 Vertices per color (*Vpc* ) of analytical model and simulations of RIC

**Fig.** 8 compares the *Vpc* of RIC with complete coloring [26-28]. Unlike RIC that keeps improving *Vpc* following the decrease of colors, the improvement of complete coloring stops at $\chi(G)$ colors, which are the minimum colors it can use. The *Vpc* of RIC has an increase of 90% over the complete coloring using $\chi(G)$ colors when the WBAN density is larger than the middle density (25 Vertices) and the coloring number is one. Another comparison with RIC in **Fig.** 8 is the optimum *Vpc* in one coloring, which is a dual problem of finding the maximum independent set (MIS)[8] in the given graph. **Fig.** 8 shows that RIC has near optimum *Vpc* at low and middle densities (12 and 25 vertices). Even at high and extremely high densities (50 and 100 vertices), RIC has a performance of around 90% compared with the MIS values.

[8] Maximum Independent Set (MIS) is defined as the maximum set of pair-wise non-adjacent vertices in a graph.

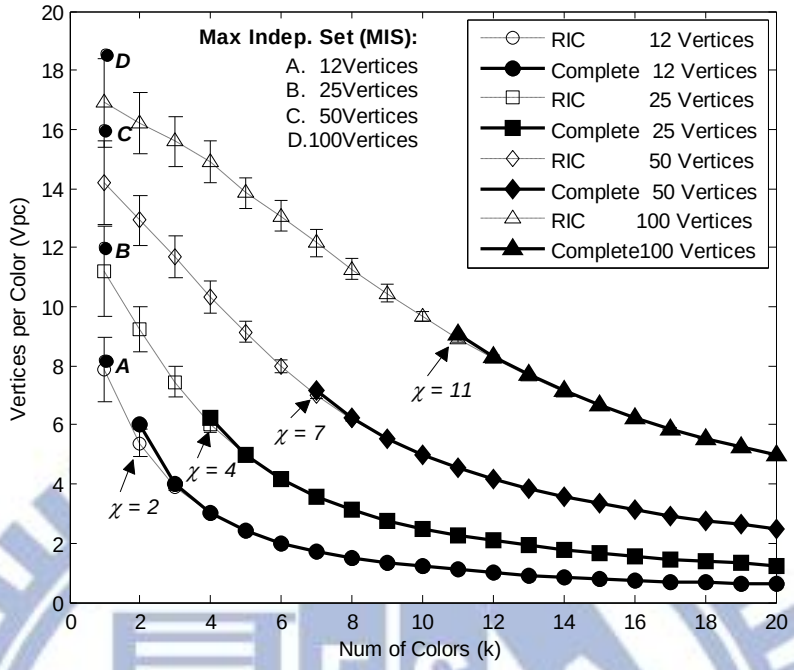


Fig. 3-8 Vertices per color (*Vpc* ) of RIC and complete colorings

## 3.4.B Performance Evaluation of CPN-based IWS

Consequently, RIC is applied in a CPN-based IWS to observe how its high coloring-speed and high spatial-reuse improve IWS performance in mobile and dense WBAN scenarios.

**Simulation Settings of Coloring-based IWS**

A proposed CPN-based IWS adopts a time division multiple access (TDMA) with two distinct communication channels: inter and intra-WBAN channels. It helps to realize and compare different kinds of coloring-based IWSs. A CPN uses both channels for inter-WBAN resource contention and intra WBAN data (vital signals) collection respectively; a WSN only uses an intra-WBAN channel for data (vital signals) transmission. Following the steps of a CPN-based IWS in section 3.1, a CPN first uses the inter-WBAN channel to contend time slots through a coloring algorithm. The CPN then sends a beacon through an intra-WBAN channel to allocate obtained time slots to its WSN. Finally,

the WSN transmits a data packet to its associated CPN through the intra WBAN-channel at the time slot that was pre-scheduled by the CPN.

The framing structure is illustrated in **Fig.** 3-9. A coloring cycle is performed for each superframe. The intra-WBAN channel consists of one beacon slot and $p$ data slots. Each CPN can reserve at most one slot after each coloring cycle. The number of data slots to be scheduled in each coloring cycle is set as $k$ (equals to the number of colors used in the coloring). The duration of each data slot is 1ms. On the other hand, the inter WBAN channel consists of $r$ slot-groups for $r$ coloring rounds in a cycle. Each coloring round has $q$ slots and is subdivided into $(q-k)$ coloring slots and $k$ winner notification slots, where $k$ is the number of colors used for coloring. Coloring slots are used for exchanging coloring messages between CPNs (e.g. **Fig.** 3-4 step 2). The CPN chooses a coloring slot in each coloring round to transmit its coloring message. The coloring slot is randomly chosen to reduce potential collisions between coloring messages. Once a CPN wins the slot (color), it broadcasts the winner message at the associated winner notification slot (e.g. **Fig.** 3-4 step 4). Because the coloring message exchanged across the inter-WBAN channel contains only color and random value information, the duration of coloring and winner notification slots are set as 25μs, which is $1/40$ of the data slot at the intra-WBAN channel. In this study, we skip the steps of superframe synchronization between CPNs, which is beyond the scope of this study. Related work on superframe synchronization can be found in [32].

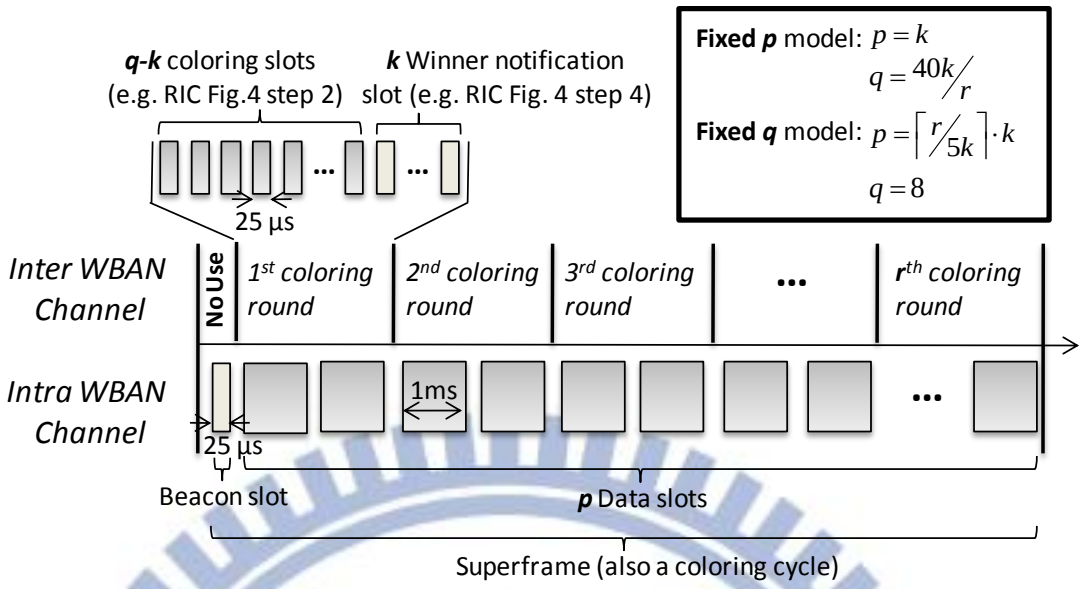


Fig. 3-9 Superframe for coloring-based IWS

The settings of $p$ (number of data slots in a superframe) and $q$ (number of coloring slots in a coloring round) are two important control variables that dominate two kinds of data collision: (1) out-of-date scheduling and (2) ill-scheduling. Out-of-date scheduling happens when the frequency of the IWS cannot catch up to the frequency of topology changes due to user mobility. The data transmissions of WSNs scheduled by the out-of-date scheduling might collide with other transmissions from un-negotiated WBANs. Because IWS is performed for each superframe, such collisions are dominated by the duration of the superframe $p$. The second kind of collision is caused by ill-scheduling, which results from the collision of coloring messages (in short, coloring collision) while CPNs broadcast their coloring messages in the same coloring slot. Without correctly receiving coloring messages from adjacent CPNs, a CPN could make a mistake on treating itself as the slot (color) winner. As a result, data transmissions of WSNs belonging to different WBANs could be scheduled to the same data slot and then collide with each other. Since coloring slots are randomly chosen by each CPN, the larger the number of coloring slots, the lower the collision rate. The number

of coloring slots is decided by the value $q$. To closely study both kinds of collisions, two types of settings are used: fixed-p and fixed-q. For the fixed-p model, $p$ is set as the number of colors $k$ (coloring numbers). Thus, each coloring round at the inter-WBAN channel has $q = 1ms/25\mu s \cdot k/r = 40k/r$, where $r$ is the number of coloring rounds. As for the fixed-q model, we choose $(k,r)=(1,5)$ to set the baseline size of $q$ as 8 slots, which introduces the most serious coloring-message collision[9] of $\varphi_{RV-INC}$. Thus, $p = 8r/40 = r/5$. Because each $k$ coloring provides $k$ slots scheduling, it is more convenient to make $p$ an integral multiple of $q_{INC-only}$. As a result, $q_{RV-INC}$ is modified as $q = 40k/r$ and the coloring result repeats every $\varphi_{INC-only}$ slots.

The generation of mobile WBAN topology is similar to the 2-D random graph. The initial positions of $n$ WBANs are randomly located in a $10\times10\,m^2$ square. $n$ can be 12, 25, 50, 100 to simulate low, middle, high, and extremely high WBAN densities. The mutually-interfering-range of WBANs is set as 2 m. Also, to simulate WBAN mobility, the location change of WBANs follows the Gauss-Markov mobility model [33]. We use [33] to simulate the smooth movement path of a human, while avoiding the sudden stops and sharp turns that happen in the random walk mobility model [34]. The Gauss-Markov mobility model has a tuning factor $\alpha$ to control the randomness of WBAN movement. $\alpha$ is set as 0.3 in this study ($\alpha=0$ and $\alpha=1$ correspond to Brownian motion and linear motion respectively).

System throughput is the performance index used to evaluate IWS. Without loss of generality, system throughput is defined as effective transmissions per slot ( *Tps* ), which counts data

[9] Fig. 6, RIC can be finished within 5 rounds $(r=5)$. While $r=5,k=1$ is the setting that yields a minimum $q$ from the equation $q = 40k/r$, which introduces the most serious coloring-message

transmissions of all WSNs that are actually received by CPNs in the system. *Tps* is similar to the vertex per color (*Vpc*) but further considers performance degradation caused by data collision.

**System Throughput of IWS**

Coloring speed is found to be the key factor that affects the performance of IWS. **Fig.** 3-10 compares the system throughput of IWS using the RIC and INC-only algorithms. INC-only can perform sub-$\chi(G)$ coloring but has a much higher time-complexity than RIC (see **Fig.** 3-6). First, in **Fig.** 3-10, ill-scheduling is temporarily ignored to make the observation of out-of-date scheduling much more clear. Because the collisions of coloring messages are ignored, the performances of RIC and INC-only in the fixed-p model are identical. Also, $r_{RIC}=5$ leads to $p_{RIC}=k$, which makes the performance of RIC in fixed-p and fixed-q models equivalent. **Fig.** 3-10 shows that the fixed-p model overcomes the mobility much better than the fixed-q model. In the fixed-q model, $p_{INC-only}=\left\lceil \frac{r}{5k} \right\rceil k$ is prolonged by the high time-complexity (high number of $r$) of INC-only and thus fails to respond in a timely fashion to topology changes. On the other hand, in the fixed-p model, $p=k$ is independent of coloring rounds $r$. Throughput is only slightly degraded while mobility is increased from 3m/s to 9m/s. Furthermore, in the fixed-p model, throughput is improved while the coloring number $k$ is decreased. This improved throughput ought to lead to more out-of-date scheduling. Fortunately, the frequency of IWS is inversely proportional to the duration of the superframe ($k+1$). Decreasing $k$ increases IWS frequency to compensate for the collisions caused by throughput improvement.

---

collision.

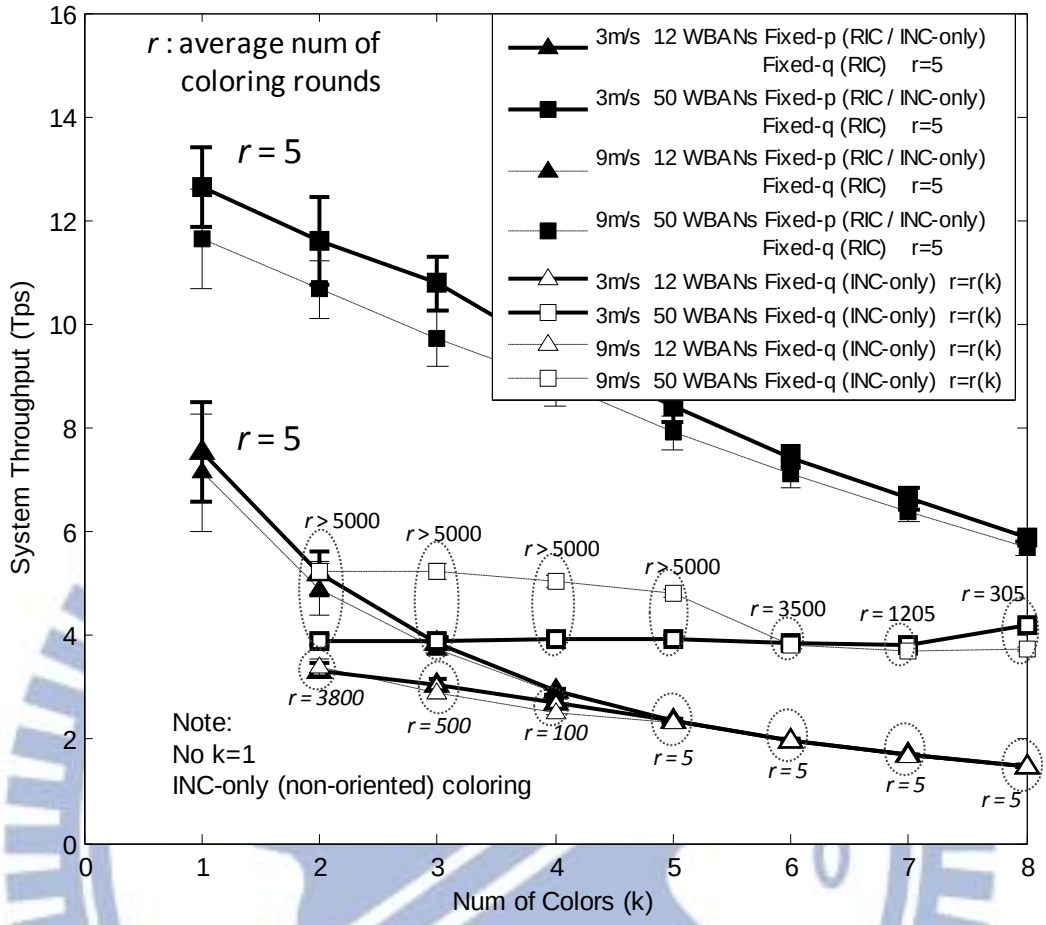


Fig. 3-10 Transmission per Slot ( *Tps* ) of IWS (ignoring ill-scheduling)

Now we focus on the fixed-p model. Ill-scheduling (coloring collision) is found to be the major factor that seriously degrades the performance of IWS. **Fig.** 3-11 illustrates the system throughput of IWS in the fixed-p model after considering both out-of-date and ill-scheduling collisions. It shows that RIC has a much higher *Tps* than INC-only. The reason comes from the substantially fewer coloring rounds of RIC than that of INC-only. $r_{INC-only}$ might be larger than thousands of slots due to the inefficient re-coloring of INC-only, which makes $q_{INC-only}$ much lower than $q_{RIC}$ ($q = 40k/r$)

and introduces serious collisions of coloring messages. For INC-only, $q = 40k/r(k)$ can be increased by increasing $k$ and decreasing $r(k)$ (coloring rounds $r(k)$ decrease while color choices $k$ increase, as shown in **Fig.** 3-6). The coloring collision of INC-only is relieved when $k$ is larger than 4 and 5 for the scenarios of 12 and 25 WBANs, respectively. However, increasing $k$ also decreases $Tps$ (referring to the decreasing $Vpc$ in **Fig.** 3-7). For RIC, the tradeoff between coloring collision and $Tps$ reduction yields optimum throughputs when $k$ is 2 and 5 (instead of 1) for the 50 and 100 WBANs cases, respectively.

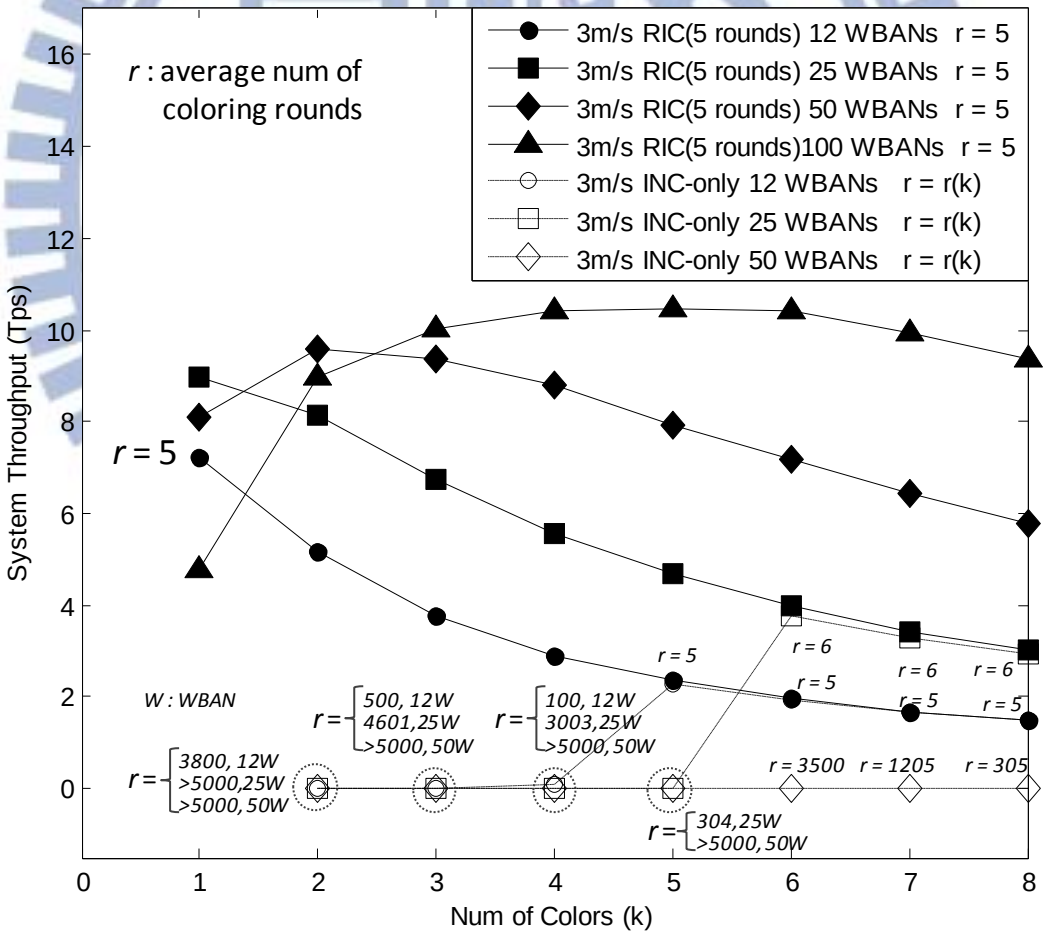


Fig. 3-11 System throughput of IWS with the Fixed-p Model

## 3.5 Summary

In this work, random incomplete coloring (RIC) is proposed to realize a fast and high spatial-reuse inter-WBAN scheduling (IWS). Unlike conventional complete coloring schemes, RIC is not limited by the tradeoff between coloring speed and spatial reuse. RIC can always provide fast convergence with time complexity $O\left(e^{W(2\ln n)/2}\right)$ in any spatial reuse requirement. Furthermore, RIC can support an increase of up to 90% of spatial reuse over the conventional complete coloring using chromatic $\chi(G)$-colors, which is known to be the optimal coloring of complete coloring. In the simulation, RIC is applied in a CPN-based IWS protocol with TDMA framing structure. Simulation results show that RIC does overcome inter-WBAN collisions and thus provides high system throughput for mobile wireless body area networks.

This study focuses on the scenario of random-user position, which is modeled as a 2-D random graph. In the future, we would like to analyze the performance of RIC in other special scenarios. For example, users in a waiting line, a movie theater, or a coffe bar. These scenarios can be modeled as a line, a grid, and a clustered graph, respectively.

# Chapter 4

# Distributed Multiuser QoS Designs

Quality of Service (QoS) for medical applications is an emerging issue for wireless body area networks (WBAN) [1, 35]. To reliably transmit data streams of medical applications (e.g. vital signals or diagnosis audio / video), WBAN QoS is asked to meet more harsh requirements than those of other wireless networks in terms of transmission latency, packet error rate (PER), and energy consumption, as mentioned in [36-42]. Furthermore, WBAN QoS is featured by considering different critical levels of vital signals. For instance, electrocardiograms (ECG) are deemed to have more important information than body temperature to indicate the health status of a person, hence ECG signals are supposed to have higher priority than that of body temperature. Many centralized scheduling technologies of medium access control (MAC) layer have been proposed to support QoS for a single WBAN (single user) [36-42]. In these works, a central processing node (CPN) of a WBAN centrally schedules radio resources of wireless sensor nodes (WSNs) illustrated in **Fig. 4-1**. These centralized controls can effectively meet various QoS requirements of vital signals. They also save energy consumptions of WSNs due to their light control loading of WSN in the CPN-centralized controls [42]. Nevertheless, some WBAN scenarios involve co-existence of multiple users, e.g. a hospital waiting room or a crowded subway station. Co-channel and co-location interference happens when WBANs move close to each other. It causes packet collisions and energy waste, which hence impact WBAN QoS. Besides, multiuser scenarios might need extra definitions of critical levels of medical data. The critical levels of vital signals might vary according to not only signal properties (like the ECGs v.s. Body temperature example in a single WBAN QoS) but also

user status. For instance, vital signals of an injured person might need higher priority than that of a healthy one. Thus, inter-WBAN priority scheme would be necessary. As a result, a new challenge of multiuser QoS that considers above inter-WBAN issues is introduced. To the best of our knowledge, there is no existing works addressing on solutions of multiuser WBAN QoS so far. Comprehensive studies are still required.

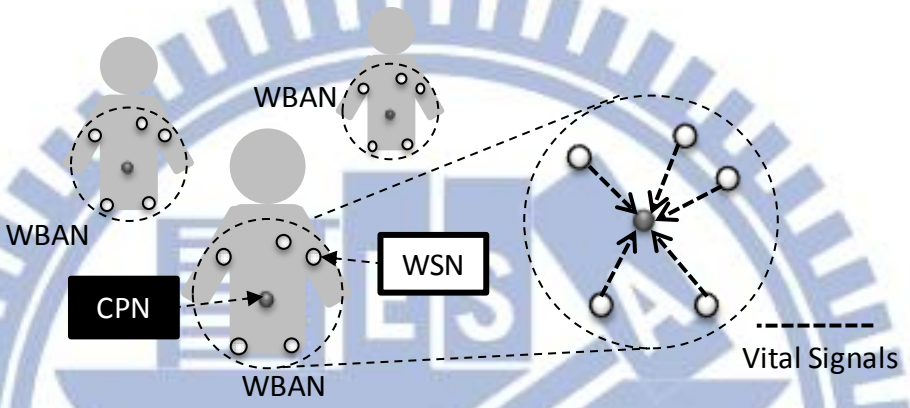


Fig. 4-1 Wireless Body Area Network

QoS designs for overlapped wireless local area networks (WLANs) or Bluetooth piconets might be the closest problems to multiuser QoS. Jiang and Howitt [43] analyze load-balancing between co-channel and co-location (overlapped) WLANs. Access points (APs) properly share bandwidth according to an optimized load-balancing through backhaul (wire-line) communications. On the other hand, for overlapped piconets, the inter-piconet interference is overcome by interconnecting discrete piconets into a scatternet [44-49]. A scatternet (cross piconet) scheduling is thus applied to provide collision free transmissions among overlapped piconets. However, these approaches might not be suitable multiuser QoS solutions for several reasons. First, these approaches are originally designed for non-medical transmissions, which have less strict QoS requirements and lack priority schemes for medical data. Furthermore, the WLAN approach focuses on static or low mobility scenarios. Its backhaul optimization is only suitable for fixed wireless nodes, which is not possible to

be applied for mobile WBANs. On the other hand, the scatternet approach introduces extra control/traffic loading and energy consumption of slave nodes (similar to WSNs in WBAN) when they serve as scatternet bridges. However, for many WBAN applications, WSNs are expected to be very low power and have a very long battery-life, e.g. an implanted pacemaker is requested to perform years heart-pacing without battery changes. Thus, neither the QoS solutions for overlapped WLANs nor piconets can be directly applied to multiuser QoS.

In this study, proposed Random Contention-based Resource Allocation (RACOON), which is extended from our previous work [50], provides a multiuser QoS scheme for mobile WBANs. RACOON is featured by:

- *Simple inter-WBAN resource allocation*, which simplifies the control overhead of inter-WBAN QoS control. Resource allocation between WBANs is decided through random-value comparisons between WBANs. In RACOON, only one broadcasting packet that carries random values will be required to complete every inter-WBAN resource contention.

- *Iterative inter/intra-WBAN QoS control*, which supports a dynamic QoS adjustment in mobile WBAN scenarios. The adjustment will consider both critical-level differences among (i) adjacent WBANs and (ii) Vital signals.

- *Hierarchy CPN/WSN resource allocation*, which utilizes the asymmetric CPN/WSN structure and thus decrease control loadings and energy consumptions of WSNs. In the hierarchy CPN/WSN resource allocation, CPN is in charge of both inter/intra resource scheduling. WSN only wakes up while it is polled by its associated CPN.

- *Probing base inter-WBAN interference detection*, which detects potential inter-WBAN interferences before actual collisions happen in both downlink (CPN to WSN) and uplink (WSN to CPN) transmissions. The interference detection avoids packet collisions and energy waste caused by WBAN mobility and hence extends battery life of WSNs.

The rest of this chapter is organized as follows: section 4.1 introduces requirements of WBAN QoS. Section 4.2 reveals the proposed RACOON multiuser QoS protocol. Section 4.3 presents the experimental results and section 4.4 concludes this chapter.

## 4.1 WBAN Quality of Services (QoS)

### 4.1.A Requirements of WBAN QoS

WBAN QoS controls that simultaneously support both intra and inter WBAN QoS are studied in this work. A WBAN consists of a single central processing node (CPN) and several wireless sensor nodes (WSNs). These WSNs collect various medical data (including vital signals from human body and diagnosis audio/video) and forward them to the CPN, which is depicted in **Fig. 4-1**. Intra WBAN QoS controls should make sure these medical data are timely transmitted by following their delay-bound and delay-variation requirements [51]. However, when total bandwidth requirements of a WBAN overflow its capacity, transmissions should be scheduled in an order from the highest-priority data to that has the lowest priority, which guarantees the QoS level of high priority data. Such priority settings are usually designed by medical experts according to their clinical experiences. For example, a heart failure could introduce much instant life risk than an abnormal body-temperature. Hence, ECG signals directly reflecting heart activity should have higher priority than that of temperature records. This kind of priority is called as **intrinsic data priority**. Furthermore, if abnormal vital signals are detected, the priorities of these signals should be

dynamically increased to be higher than those of normal signals. Such priority is called as **emergent data priority**. Therefore, intra WBAN QoS controls should meet various latency requirements of difference medical data and follow proper intrinsic and emergent data priorities simultaneously.

On the other hand, for inter-WBAN QoS designs, proper **user priority** should be further provided. In scenarios of multiple overlapped WBANs, WBANs need to share radio resource with each other. Once the overall capacity is not sufficient to support all transmission bandwidth of WBANs, radio resources should be allocated to WBANs that has higher user priority. Such priority should also be defined by medical experts. Usually, priority settings follow an order from the highest to the lowest life-critical WBAN users. High user-priority WBANs should be allowed to transmit all necessary medical data; low user-priority WBANs should transmit only partial medical data to maintain normal health monitoring. As a result, WBAN QoS controls should simultaneously satisfies (i) intrinsic data priority (ii) emergent data priority and (iii) user priority for both intra and inter WBAN QoS.

Aside from transmission qualities above, a WBAN QoS control should try to lower energy consumption of WSNs as well [1, 51, 52]. In a WBAN, a CPN will most likely be embedded in personal devices such as cellular phones or PDAs with larger and rechargeable batteries. In contrast, WSNs are expected to be light weight (small battery) and even un-rechargeable for certain implantable applications. Thus, WSNs are expected to keep their energy consumptions as low as possible.

### 4.1.B Performance Metrics

To qualify a QoS control for WBAN, following performance metrics will be evaluated.

- Transmission Latency: transmission latency affects smoothness of real-time display of vital signals. A transmission latency of a medical packet is calculated from the time of a packet is generated in a WSN to the time of the packet is successively received by a CPN. To ensure a vital signal is timely displayed, every packet of the signal should be received before its delay bound expires.

- Joule per bit of WSN: energy consumption of a WSN affects its battery life. To evaluate energy consumptions of WSNs with various traffic loading, an energy measurement is normalized by its transmission bandwidth with the unit, Joule per bit. An energy measurement of a WSN will count all its packet transmissions (successful/unsuccessful packet transmissions from WSN to CPN) and receptions (successful/unsuccessful polling message receptions from CPN to WSN).

- User capacity: user capacity affects the density of coexistence WBAN users, which is important for dense WBAN scenarios. User capacity is defined as the maximum number of coexistence WBANs that satisfy desired WBAN QoS requirements.

### 4.1.C Related Works

Significant contributions toward high quality WBAN QoS designs have been made in recent years [36-41, 53, 54]. These works adopt different framing, scheduling, and novel hardware techniques to optimize emergency transmission, packet latency, and power consumption of a single user WBAN. *Huasong* [38] creates a framing-structure-turning procedure to simultaneously improve throughput, queuing delay, and energy consumption of IEEE 802.15.4, a candidate protocol for WBAN. *Yoon* [36] further modifies the framing structure of 802.15.4 to remarkably reduce the packet delay of

emergency alarm. He further introduces a preemptive scheduling to guarantee the transmission priorities of various medical data. There are also scheduling techniques utilizing TDMA-overhead-reduction [53], adaptive duty cycle [54], prioritized retransmission [39], delayed retransmission [37], fuzzy-logic controls [41], and wake-up radio [54] to enhance WBAN QoS. *Su and Zhang* further combine scheduling with realistic battery charging/discharging effect to significantly prolong battery life of WBAN sensors. More complete introductions and comparisons of existing WBAN QoS solutions are summarized by *Ullah* [52]. Different from above single WBAN solutions, proposed RACOON protocol puts more focus on multi-user WBAN QoS solution, which will be introduced in following sections.

## 4.2 Random Contention-based Resource Allocation (RACOON)

The proposed Random Contention-based Resource Allocation (RACOON) is a bandwidth control system embedded in medium access control (MAC) layer for multi-WBAN QoS, which consists of two major designs: a CPN-based resource allocation and a random contention-based inter-CPN negotiation.

### 4.2.A CPN-based Resource Allocation

The CPN-based resource allocation of RACOON is designed to minimize energy consumptions of WSNs and early detect inter-WBAN interference to avoid unnecessary packet collisions. The proposed CPN-based protocol has a two-step resource allocation scheme, which is illustrated in **Fig. 4-2**. There are two distinct channels for inter and intra-WBAN communication, respectively. The inter-WBAN channel is used to exchange the resource negotiation messages between WBANs. Only CPNs can access the inter-WBAN channel. On the other hand, the intra-WBAN channel is used to transmit polling messages from CPN to WSN and data packets from WSN to CPN. The superframe

is divided into fixed number of slots. Each slot is sub-divided into a short polling slot and a data slot, which are illustrated in **Fig.** 4-2. WSN receive not only transmission schedule from polling messages but also framing structure information including the start of a superframe and number of slots in it. When multiple WBANs overlap with each other, a CPN first negotiates WBAN resources with adjacent CPNs through the inter-WBAN channel. The detailed procedure of inter-CPN negotiation will be introduced in section 4.2.B. The CPN then assigns reserved resources to its WSNs by polling messages through the intra-WBAN channel. As a result, the WSNs wake up only when (1) receiving polling messages from the associated CPN in polling slots and (2) transmitting vital signals to that CPN if they are polled, hence energy consumptions of the WSNs can be reduced.

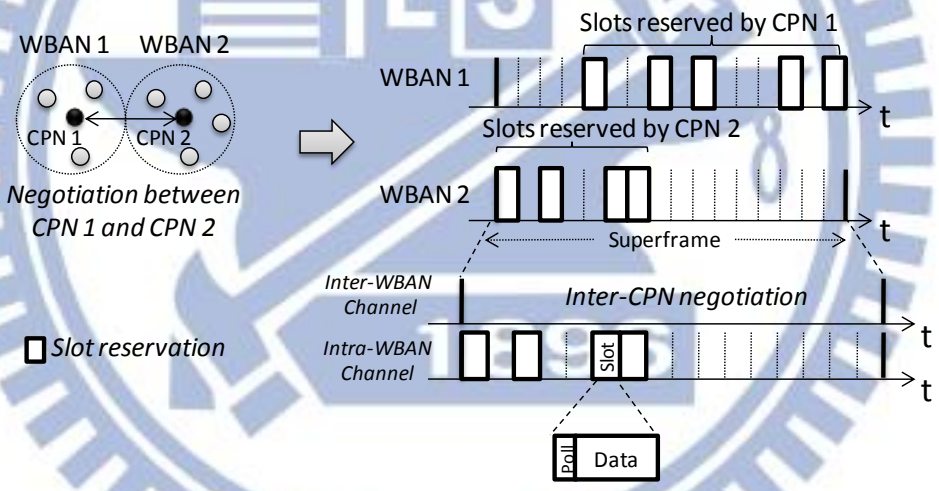


Fig. 4-2 CPN-based resource allocation of RACOON

In the proposed CPN-based resource allocation, WSNs do not need to perform any interference detection. Instead, a probing-based interference detection, which utilizes a coverage difference between CPN and WSNs, is used and illustrated in **Fig. 4-3**. A CPN has a larger transmission range than that of WSNs, which allow the CPN to detect potential interferences to its uplink (WSN to CPN)

and downlink (CPN to WSN) transmissions. The detection is realized by periodic "probing" from the CPN to its adjacent CPNs. These probing messages are exactly the inter-CPN negotiation messages and the CPN is probed when it receives negotiation messages from other CPNs. Therefore, the interference detection and inter-WBAN negotiation are finished at the same time. **Fig. 4-3** illustrates the proper range settings of a CPN and a WSN. For example, in an uplink (WSN to CPN) transmission with WSN' as the source of interference (Soi), which is shown as case (a) in **Fig. 4-3**, CPN (CPN') and WSN (WSN') have the transmission ranges $R_{CPN}$, and $R_{WSN}$, respectively. For simplicity, the range of possible WSN position is assumed as a cylinder and shadowing effects of human body are ignored. CPN is located at the center of cylinder and WSNs are located within the cylinder. In case (a), a data packet is transmitted from WSN to CPN. In the mean time, WSN' is transmitting data as well. To avoid a data collision happens at CPN, the distance from the interference edge of WSN' (Soi) to CPN (Rx), that is, $D_{Esoi2Rx} = \left|\overrightarrow{W'C}\right| - R_{WSN}$ should be positive. Because the location of WSN' is confined by the cylinder, the minimum $\left|\overrightarrow{W'C}\right|$ lies on the $\overrightarrow{C'C}$ connection. For this reason, the minimum $R_{CPN}$ that makes $\left|\overrightarrow{W'C}\right| - R_{WSN}$ positive should be larger than $R_{WSN} + d/2$, where $d$ is the diameter of the cylinder. CPN thus can detect the neighbor WBAN from radio activities of CPN' before the interference of case (a) happens. Results of other combination of possible transmission directions and sources of interference are also presented in **Fig. 4-3**. By considering all cases, $R_{CPN}$ should be at least larger than $R_{WSN} + d$ to ensure collision free transmissions.

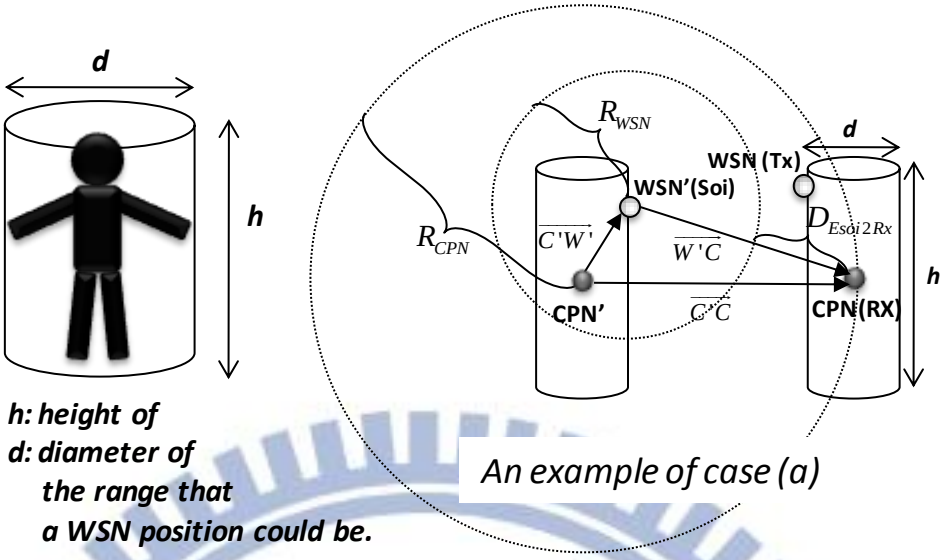


| Tx→Rx | | Soi | $D_{Esoi2Rx}$ | Condition that CPN detects interf. from Soi with Cylinder Model |
|---|---|---|---|---|
| (a) | WSN→CPN (Uplink) | WSN' | $\left\|\overrightarrow{W'C}\right\| - R_{WSN}$ | $R_{CPN} > R_{WSN} + d/2$ |
| (b) | | CPN' | $\left\|\overrightarrow{C'C}\right\| - R_{CPN}$ | N/A $*R_{CPN} = \left\|\overrightarrow{C'C}\right\|$ |
| (c) | CPN→WSN (Downlink) | WSN' | $\left\|\overrightarrow{W'W}\right\| - R_{WSN}$ | $R_{CPN} > R_{WSN} + d$ |
| (d) | | CPN' | $\left\|\overrightarrow{C'W}\right\| - R_{CPN}$ | $R_{CPN} > R_{WSN} + d/2$ |

Fig. 4-3 Probing-based interference detection

## 4.2.B Random Contention-based Inter-CPN negotiation

The inter-CPN negotiation of RACOON is an iterative bandwidth control scheme adjusted by two parameters: **Bandwidth Requirement** and **User Priority Index**. These two parameters are calculated by each CPN according to the status of it associated WSNs. From **Fig. 4-4**, each WBAN iteratively contends wireless resources to achieve a pre-defined bandwidth target. Besides, to reflect the emergency level (user priority index) of WBAN, two trends of bandwidth control scheme are provided for high and low priority WBANs, respectively. High priority WBANs aggressively contend resources to achieve a high bandwidth target, $BW_{Desire}$. Bandwidth requirements of a low priority WBANs are relaxed to be in between $BW_{Desire}$ and a lower target $BW_{Require}$. Thus, when

high and low priority WBANs contend to each other, high priority WBANs are expected to achieve better bandwidth targets than those of low priority WBANs can achieve.

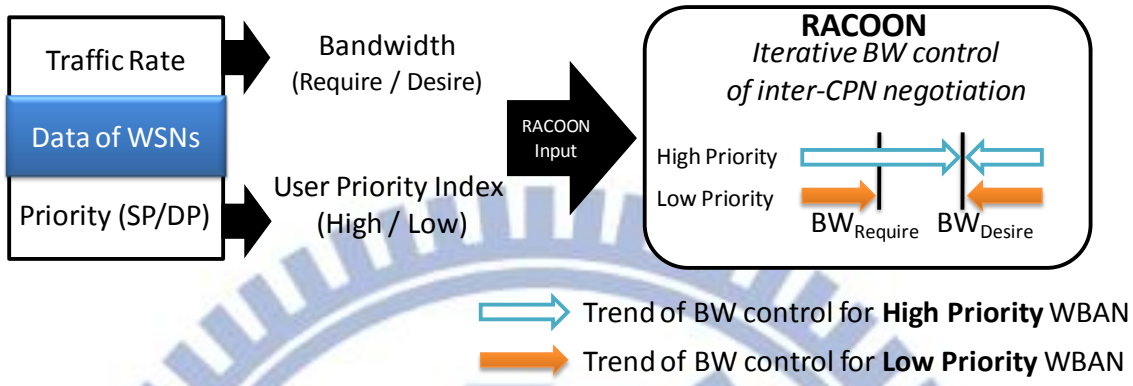


Fig. 4-4 Random Contention-based Inter-CPN negotiation of RACOON

The calculation of the bandwidth target, $BW_{Desire}$, $BW_{Require}$, and User Priority Index depends on proposed priority system for WSN. Each WSN has two kinds of priority indexes: static priority (SP) and dynamic priority (DP). Both SP and DP are set to either 0 (low) or 1 (high) depending on its intrinsic and emergent data priorities mentioned in section 4.1. SP represents the importance of monitored signal. DP denotes the emergency level when a value of a monitored signal is out of its normal range.

$BW_{Require}$ is defined as the minimum resource that a WBAN requires to transmit its emergency data, that is, $BW_{Require} = \sum_i BW_i, (\forall i \in W) \cap (DP_i = 1)$, where $W$ is the set of WSNs in a WBAN; $DP_i$ is the dynamic priority of $WSN_i$. On the other hand, $BW_{Desire}$. is defined as the bandwidth that a WBAN needs to transmit both emergency and non-emergency data, that is,

$BW_{Desire} = \sum_i BW_i, \forall i \in W$. As for the User Priority Index, it is decided by comparing the ratio of the number of emergency WSNs over all WSNs with a pre-defined threshold of User Priority Index, which are $|E|/|W|, E = \{\forall i \subset W \cap DP_i = 1\}$ and $UPI_{th}$ respectively. When $|E|/|W| > UPI_{th}$, it is a high priority WBAN, otherwise, it is a low priority WBAN. Usually, $UPI_{th}$ is a personal configuration and is expected to be defined by medical experts by considering syndromes and associated sensors of a WBAN user.

In RACOON, with the inputs of $BW_{Desire}$, $BW_{Require}$, and User Priority Index, each CPN generates a weighted random value to contend resources with its neighbor CPNs. The scheme of weighted random value is inspired by Neighborhood-aware Contention Resolution (NCR) algorithm [55], which provides collision free scheduling. The skill of NCR is a random value comparison scheme. Each wireless node first generates a random value. The wireless node that has the largest random value wins the transmission slot. As for the weighted random value contention in our case, it can be realized by a pseudo contention. A CPN first generates its $N_{rnd}$ uniform random values and picks the largest one for a slot contention. The average probability $P_i$ that CPN $i$ can obtain a slot is proportional to the number of random values, $N_{rnd_i}$, used in the pseudo contention. That is

$$P_i = \frac{N_{rnd_i}}{\sum_{j, j \in N(i) \cup i} N_{rnd_j}} \quad (4\text{-}1)$$

where $N(i)$ is the set of neighbors of CPN $i$. With this skill, each CPN iteratively controls its $N_{rnd}$ to achieve their bandwidth targets according to the control flow illustrated in **Fig. 4-5**. At the start of each contention iteration, the available bandwidth $BW_{Avb}$, which is defined as the bandwidth

that a WBAN has in its previous iteration, is compared with its two bandwidth targets, $BW_{Desire}$ and $BW_{Require}$. Then a three-case decision is decided basing on that:

Case 1: $BW_{Avb} < BW_{Require}$

Case 2: $BW_{Require} \leq BW_{Avb} \leq BW_{Desire}$

Case 3: $BW_{Desire} < BW_{Avb}$

The value of $N_{rnd}$ will be changed based on the priority setting of a WBAN. As shown in **Fig. 4-5**, high-priority WBANs are designed to increase their $N_{rnd}$ more aggressively than those of low-priority WBANs. Thus, the high priority WBANs are more possible to achieve their bandwidth requirements than the low priority WBANs. In the proposed design, an iteration of contention is performed in a superframe. A CPN first generates random values for all slots according to $N_{rnd}$ respectively and broadcasts only one negotiation message carrying these values through the inter-WBAN channel to its adjacent CPNs. Thus, contentions can be performed by value comparisons between CPNs. To avoid collisions between negotiation-messages, these messages are broadcasted at random time slots within a superframe.

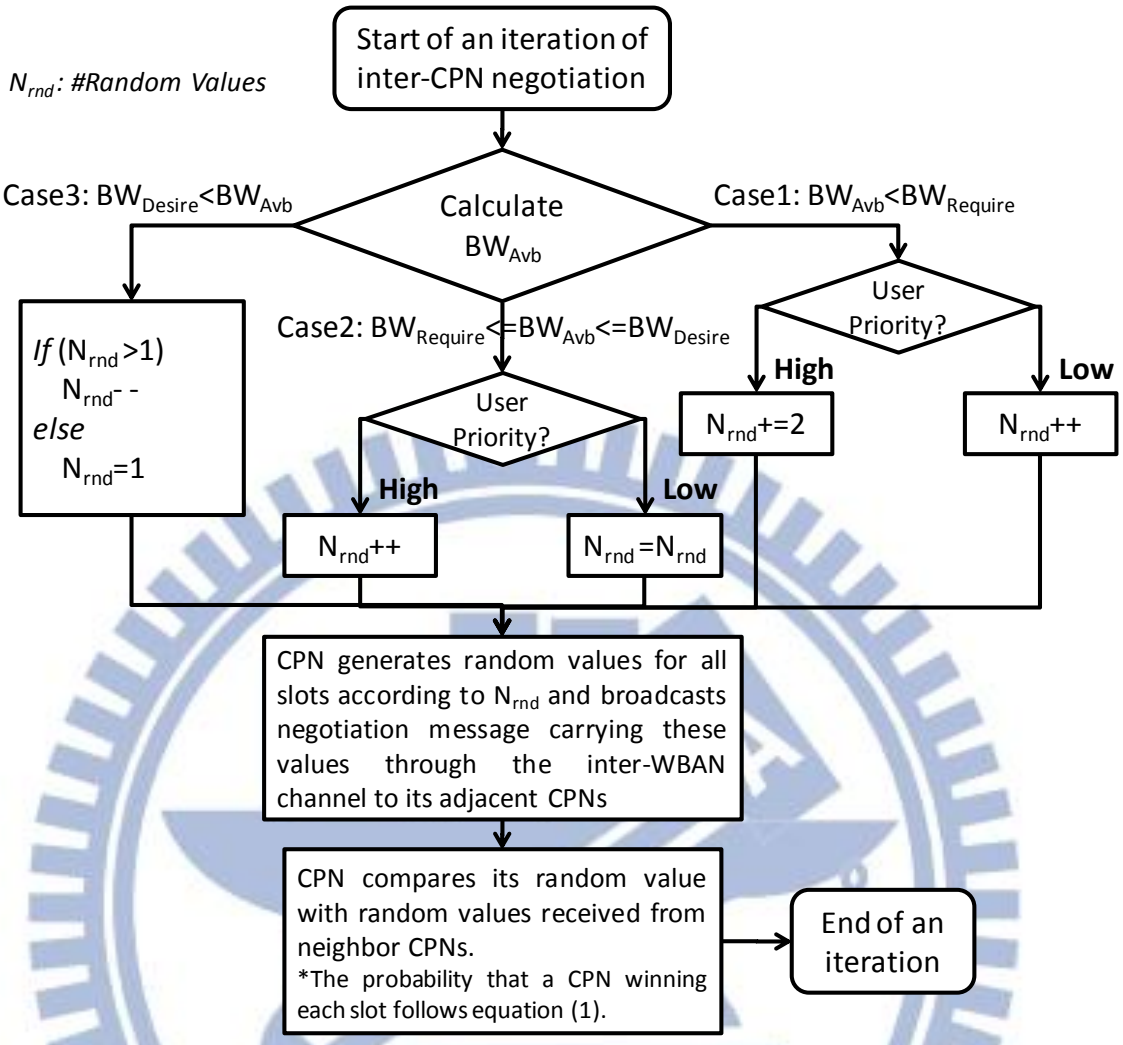


Fig. 4-5 Bandwidth control flow of inter-CPN negotiation in RACOON

After a CPN finish an inter-WBAN resource contention, it performs an intra-WBAN scheduling to allocate its reserved transmission slots to its WSNs. A multi-queue scheduler is adopted to schedule resource by following order from the WSN that has the highest value of SP+DP to that has the lowest value, which is depicted in **Fig. 4-6**. A data in a queue is scheduled only when there is no data in other queues that has higher SP+DP value.

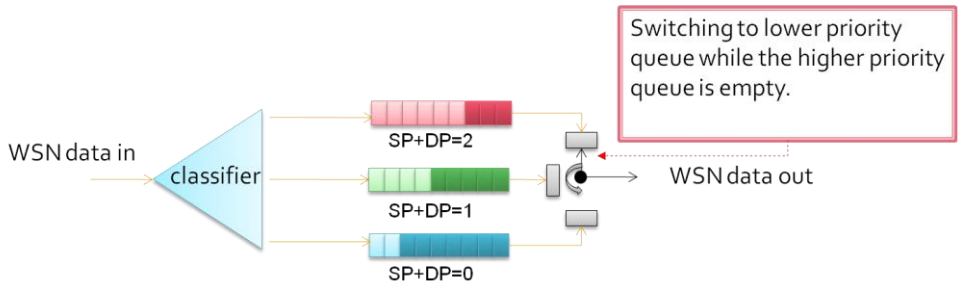


Fig. 4-6 Multi-queue scheduler of intra-WBAN scheduling

## 4.3 Computer Simulation

### 4.3.A Benchmarking WBAN QoS Protocol

BodyQoS [42] is a MAC layer scheduling scheme chosen to benchmark the proposed WBAN QoS protocol. BodyQoS is a CPN-centralized single-WBAN-QoS control that is capable of overcoming performance impacts from co-channel interference. The design strategy of BodyQoS is to increase transmission opportunities of a WSN when it suffers a bad channel condition. The transmission opportunity is inversely proportional to its available bandwidth, hence a vital signal can be timely transmitted without extra delay. The bandwidth control of BodyQoS can be expressed as:

$$\frac{TxOpportunities(t)}{TxOpportunities_{ideal}} = \frac{BW_{ideal}}{BW_{Avb}(t-1)} \tag{4-2}$$

$$BW_{Avb}(t-1) = \alpha \cdot BW_{Measured}(t-1) + (1-\alpha) \cdot BW_{Avb}(t-2)$$

where $BW_{ideal}$ is the ideal bandwidth with perfect channel; $BW_{Avb}$ is calculated by a moving average of previous measured bandwidth $BW_{Measured}$. To fairly compare the BodyQoS with the

proposed RACOON protocol, bandwidth measurement of the BodyQoS is performed every superframe. Besides, to avoid unpredictable interference, transmission opportunities are randomly scheduled within every superframe.[10]

### 4.3.B Experimental Settings

A MATLAB simulation platform is built to evaluate the proposed RACOON protocol. Detail settings of topology, PHY radio, MAC framing, and traffic loads, are listed in table I. Besides, to simulate WBAN mobility, the location change of WBANs follows the Gauss-Markov mobility model [33]. We use [33] to simulate the smooth movement path of a human, while avoiding the sudden stops and sharp turns that happen in the random walk mobility model [34]. The Gauss-Markov mobility model has a tuning factor $\alpha$ to control the randomness of WBAN movement. $\alpha$ is set as 0.5 in this study ($\alpha = 0$ and $\alpha = 1$ direct to a Brownian motion and linear movement respectively).

[10] The original interference-avoidance scheme of BodyQoS is a Carrier Sense Multiple Access with Collision Avoidance (CSMA/CA) protocol. A random scheduling is used to simulate the random backoff skill of CSMA/CA.

TABLE 1 Experimental Setting of WBAN QoS

| Item | Value | | |
|---|---|---|---|
| **Framing structure** | 10 slots per superframe / each slot is 50ms long | | |
| **Packet size** | 240bytes | | |
| **Transmission rate** | 48kbps | | |
| **RX Power** | 27.3mW | | |
| **TX Power** | 31.2mW | | |
| **Topology** | 1 to 10 WBANs randomly deployed in a 6x6m$^2$ square. When number of WBANs is more than one, the ratio between high and low priority WBANs is 1:1. | | |
| **Transmission range** | Distance between CPN and WSN: 0.5m. Referring to the range settings of probing-base interference detection in section 4.2.A, CPN: 3m / WSN: 2m. | | |
| **Data Type** | **Data Rate** | **Data Priority (SP, DP)** | **Delay Bound** |
| **ECG ch1** | 4kbps | 1, 1 | 1s |
| **ECG ch2** | 4kbps | 1, 1 | 1s |
| **SpO2** | 3kbps | 1, 0 | 1s |
| **Blood pressure** | 3kbps | 0, 1 | 10s |
| **Temperature** | 2kbps | 0, 0 | 10s |
| **Heart rate** | 2kbps | 0, 0 | 10s |

## 4.3.C Experimental Results

Packet latency of different vital signals in **Fig. 4-7** illustrate how intra and inter WBAN priorities are realized in RACOON. For either high or low priority, latency of vital signals are ranked in order of SP+DP. Signal with higher SD+DP value should have lower latency. Note that SP and DP reflect the **intrinsic** and **emergent data priorities**, respectively. Furthermore, due to that the high-priority WBAN contends resources more aggressively than the low-priority WBAN does, same signal with same priority setting in the high-priority WBAN has shorter latency than that in the low-priority WBAN. This meets the QoS requirements of the **user priority**.

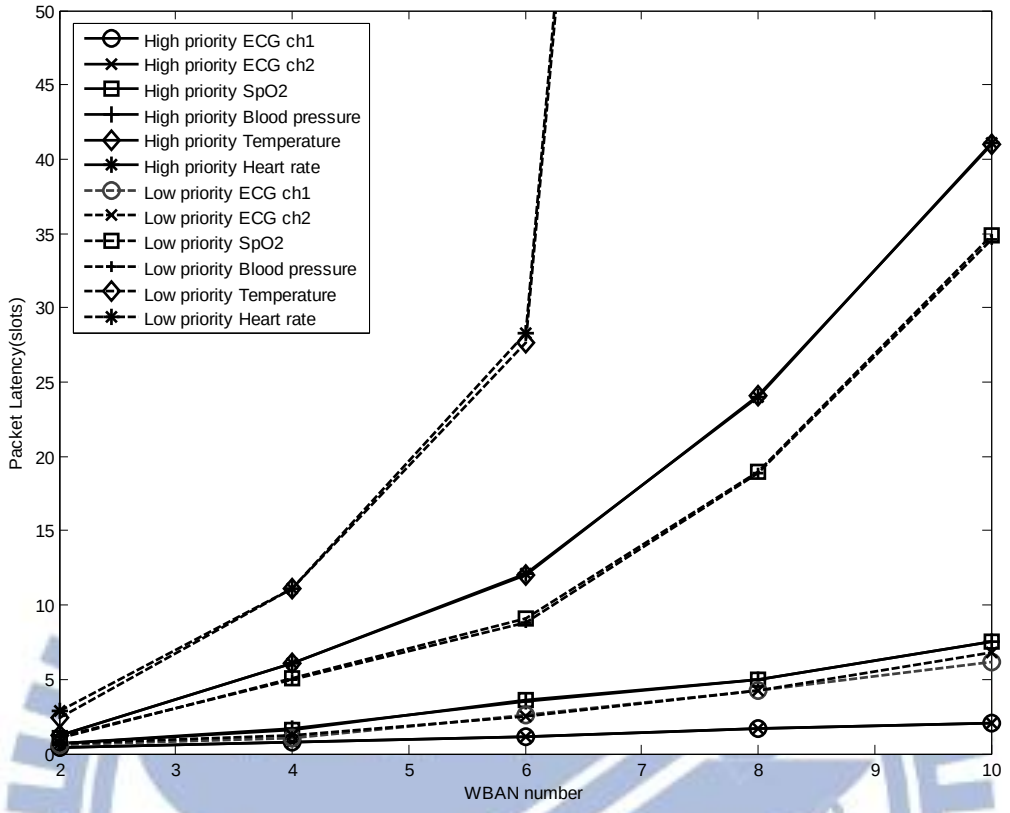


Fig. 4-7 Packet latency of vital signals in high and low priority WBANs

The latency comparison between RACOON and BodyQoS [42] in mobile WBAN scenarios is shown in **Fig. 4-8**. RACOON has much lower packet latency than BodyQoS has when WBANs move at either 2m/s or 6m/s. The reason is that RACOON makes WBANs cooperatively share the radio resource when they overlap to each other. On the contrary, BodyQoS does not consider interference interactions between WBANs, which makes improper decisions of bandwidth control and thus induces high transmission delay. In the original ideas of BodyQoS, interference is assumed to be generated by regular co-channel communications or path-loss due to limb movements. These sources of interference have "passive" interference patterns, which means it does not increase or

decrease its interference level following the bandwidth control of BodyQoS. Therefore, BodyQoS reasonably increases transmission opportunities to overcome bad channel conditions. However, in multi-WBAN scenarios, the increasing transmission opportunities cause serious inter-WBAN interference. It than increases the transmission opportunities again and causes more serious interference, which enters a vicious circle. Collision measurements with RACOON and BodyQoS in **Fig. 4-9** echo this observation.

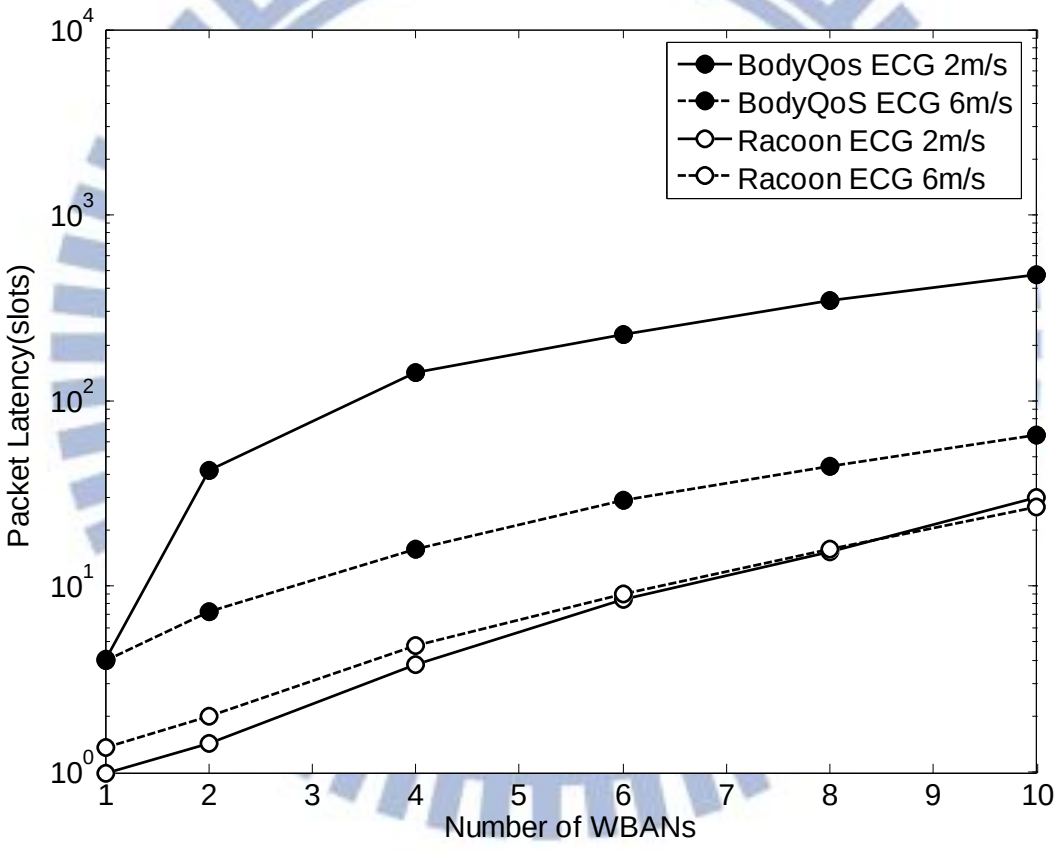


Fig. 4-8 Packet Latency with RACOON and BodyQoS

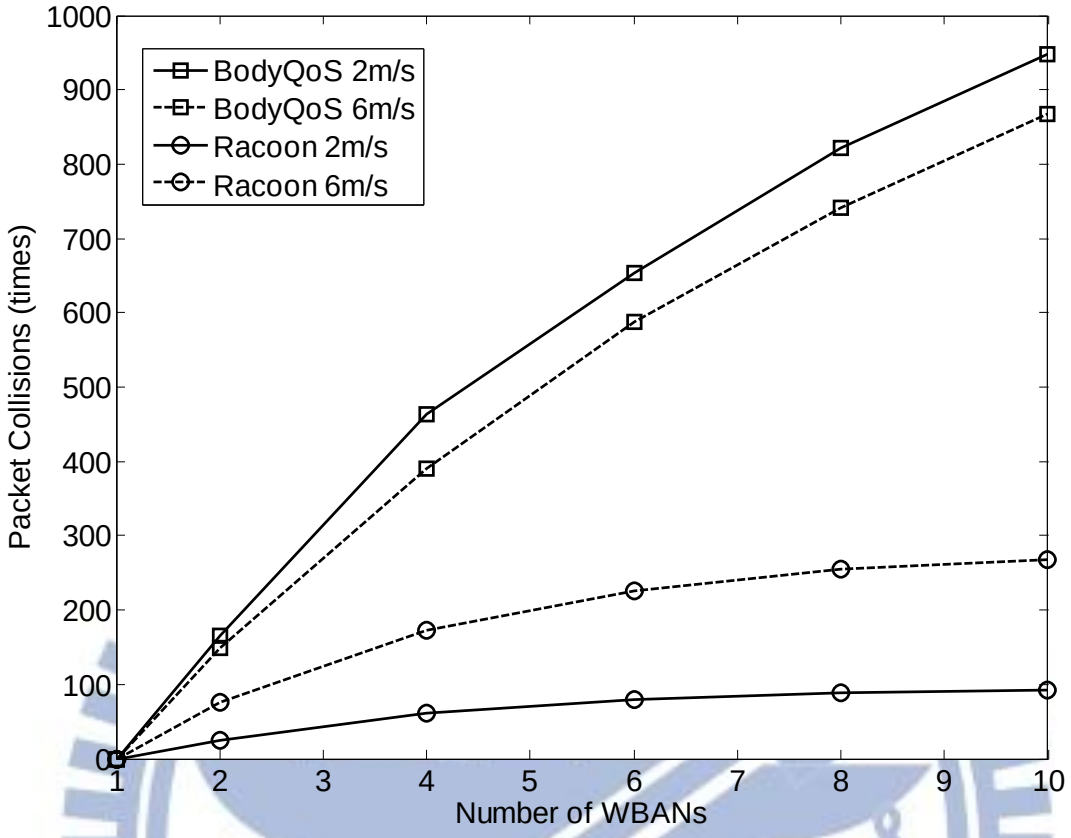


Fig. 4-9 Packet collisions with RACOON and BodyQoS controls

The collision measurements also show that collision of WBAN with RACOON is less sensitive to the number of co-existence WBANs, as compared with BodyQoS. Interference between WBANs is overcome by RACOON's cooperative inter-WBAN resource sharing scheme and proposed probing-based interference detection. Collisions of RACOON are created by out-of-date scheduling. A WBAN moves and encounters other un-negotiated WBANs with out-of-date inter-WBAN scheduling and thus packet collisions happen. However, besides of collisions created by WBAN mobility, BodyQoS creates extra collision by its problem of the inter-WBAN-interference enhancement. This problem gets worse when number of co-existence WBANs increases and hence

introduces more collisions. The difference reasons of collisions of RACOON and BodyQoS are also reflected in their energy consumptions, which is depicted in **Fig. 4-10**. Note that the energy consumption is normalized to transmission throughput. The energy consumption considers both TX and RX according to the definition in performance metrics, section 4.1.B.

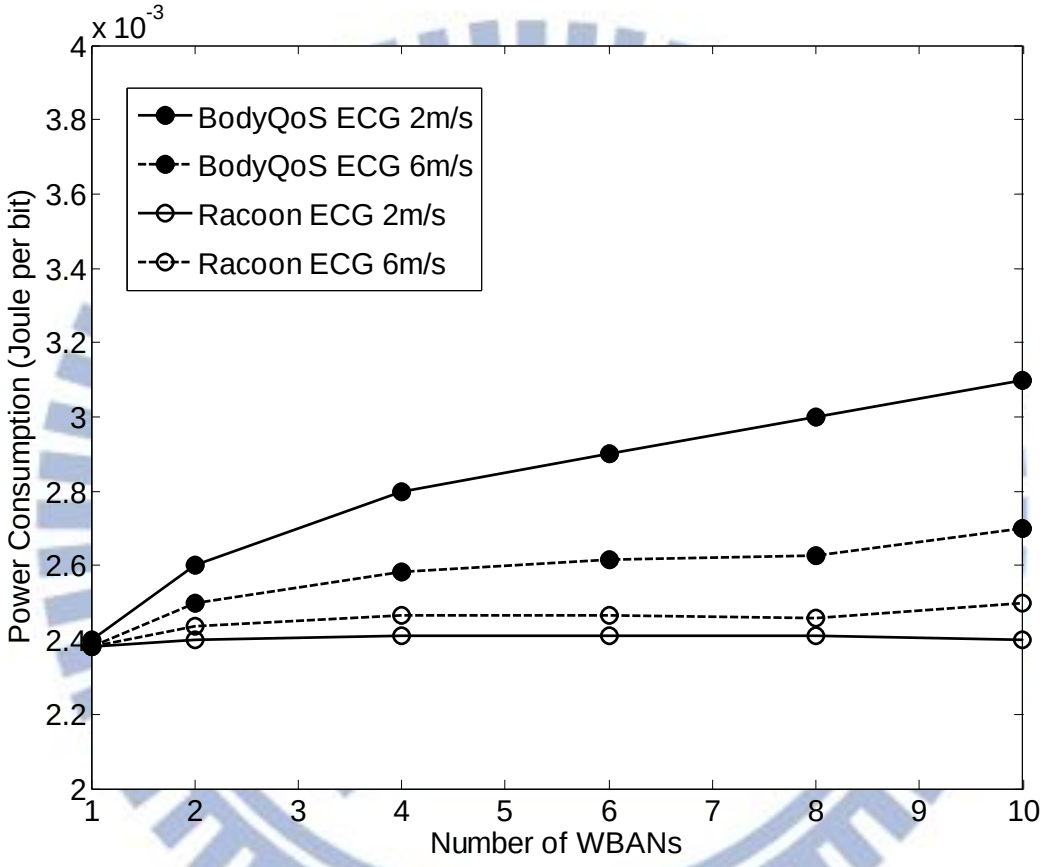


Fig. 4-10 Energy consumption of WSN with RACOON and BodyQos

There is an interesting result in **Fig.** 4-8, 4-9, and 4-10. While mobility of WBAN user is increased, BodyQoS and proposed RACOON have opposite reactions. For BodyQoS, the latency, collision, and energy consumption of a WBAN are decreased. On the contrary, for RACOON, those of a WBAN are increased, which are shown in **Fig.** 4-8, 4-9, and 4-10. The reason comes from the

different anti-interference strategies of them. As for BodyQoS, a WBAN increases its transmission opportunities when it suffers inter-WBAN interference. If a collision history of a WBAN is separated into collision and non-collision, it will form an iterative collision / non-collision / collision / non-collision … pattern. Thus, for BodyQoS, a WBAN first senses collision and tries to increase its TX times. When the TX times are increased and the WBAN moves into a non-collision area, the latency, collision, and energy consumption of a WBAN are decreased. And then this WBAN starts to decrease the TX times because it senses no interference in the non-collision area. While the TX times are decreased and the WBAN happens to move into a collision area, some collisions are avoided. As a result, for BodyQoS, mobility helps a WBAN to decrease its latency, collision, and energy consumption. RACOON has an opposite strategy in TX-times control. For RACOON, a WBAN tries to decrease its TX times (through inter-WBAN resource negotiation) to resolve inter-WBAN collision and increase the TX times when there is no collision. RACOON thus has an opposite collision result during the iterative collision / non-collision pattern. As a result, RACOON introduces more collision to a WBAN when its mobility is increased. Although mobility helps the performance of BodyQoS and decreases that of RACOON's, RACOON still guarantee a WBAN to have lower latency, collision rate, and energy consumption than what BodyQoS does due to RACOON's cooperative inter-WBAN resource allocation.

User capacity is calculated by counting number of co-existence WBANs that provide delay-bound-satisfied transmissions of corresponding vital signals, which is illustrated in **Fig. 4-11**. The proposed QoS protocol, RACOON, provides up to four co-existence WBANs that guarantee delay-bound requirements of all traffics. Its user capacity can be increased to ten co-existence WBANs when only the delay-bound of ECG traffics are satisfied. On the contrary, BodyQoS can support only single WBAN QoS due to its problem of inter-WBAN-interference enhancement.

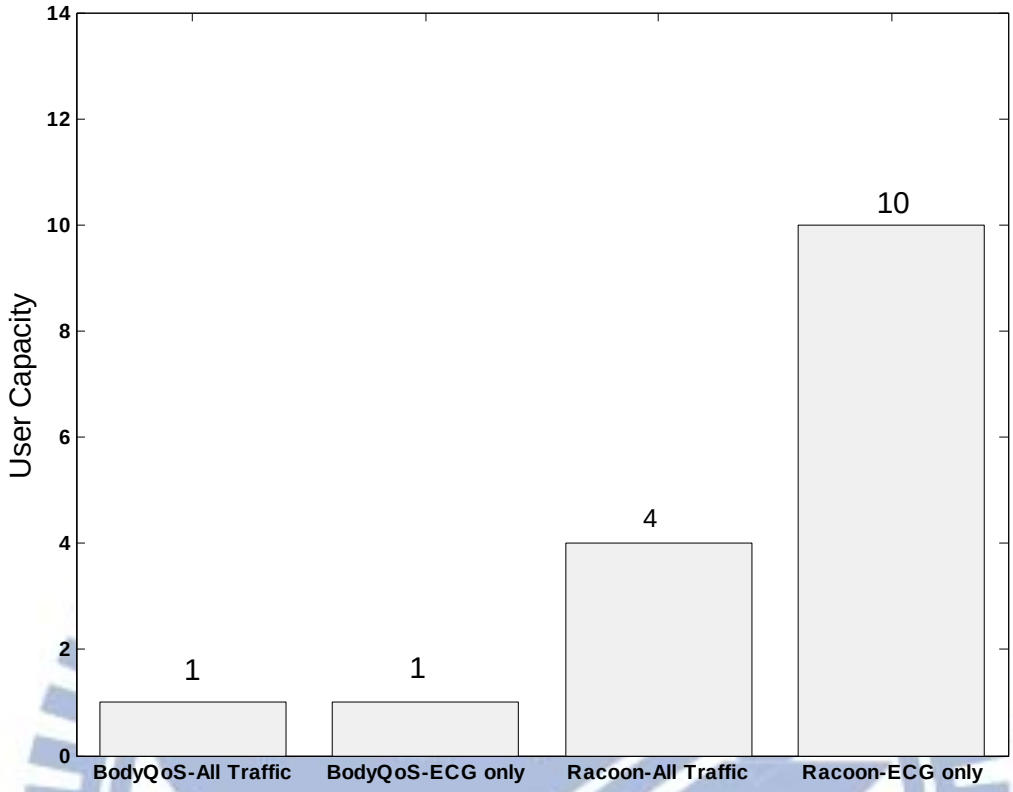


Fig. 4-11 User Capacity with RACOON and BodyQoS

## 4.4 Summary

This work proposes Random Contention-based Resource Allocation (RACOON) protocol to provide multiuser QoS for wireless body area networks (WBANs). By considering QoS requirements of practical medical applications, the inter-WBAN scheduling should have QoS controls that simultaneously consider three different priorities: (i) intrinsic data priority, (ii) emergent data priority, and (iii) user priority. The proposed RACOON protocol uses a dynamic weighted-random-value-comparison scheme to meet these priority requirements. Furthermore, RACOON utilizes a centralized control and a probing-based inter-WBAN interference detection to simplify QoS controls of wireless sensor nodes (WSNs), which decreases unnecessary energy waste of WSN. Simulation results shows that RACOON has better QoS performance in terms of

transmission latency, energy consumption, and user capacity, as compared with other WBAN QoS controls that do not consider inter-WBAN interference and priority.

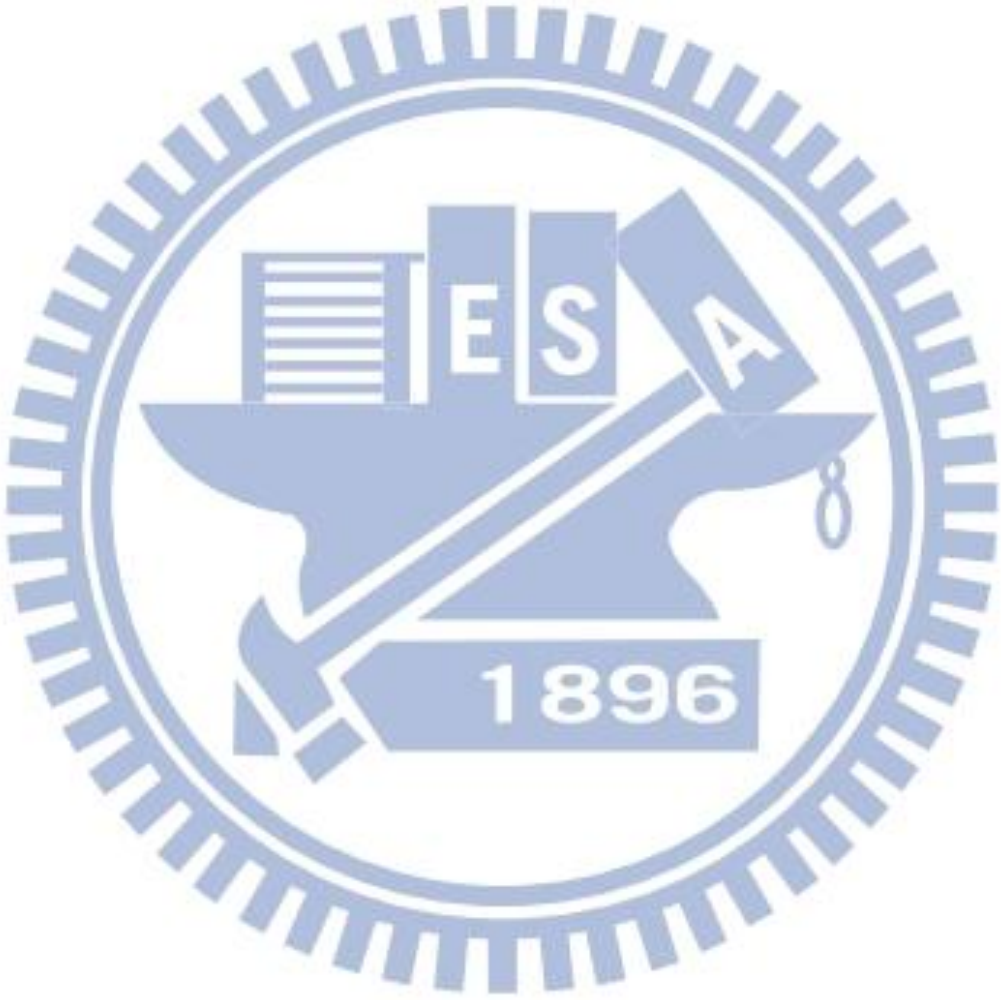

# Chapter 5

# Conclusions and Future Work

Wireless Body Area Network (WBAN) retrieving vital signals from our body has been treated as the “last meters” of the ubiquitous healthcare. To provide reliable transmission of body signals, WBAN need to overcome a WBAN-specific issue, “inter-WBAN interference”, which is caused by the mobility of WBAN users. It not only impacts the channel efficiency of WBAN but also raise a complex and WBAN-specific priority scheme.

## 5.1 Conclusion Remarks

In chapter 2, throughput and energy consumption models for multiuser WBAN are built. These models show how inter-WBAN interference degrades the performance. It also shows the performance sensitivity to the intra / inter-WBAN interference by two popular resource scheduling skills: CSMA-CA and beacon (contention free) modes. CSMA-CA properly handles the inter-WBAN interference by its random access scheme. However, it sacrifices great channel efficiency. On the other hand, beacon mode optimizes the intra WBAN scheduling but has no resistance of inter-WBAN interference. This hints the possible WBAN MAC should be a hybrid way of these schemes.

Chapter 3 further considers the dynamic topology of WBANs due to user mobility. It points out the fast response time of WBAN scheduling is another key of WBAN MAC design. Nevertheless, according to traditional graph coloring theory, channel efficiency and scheduling efficiency are tradeoffs. Chapter 3 proposes a relaxed coloring scheme combining random coloring skill to skip

these tradeoffs. Surprisingly, The proposed method not only simultaneously realize high channel efficiency and scheduling speed but also has even higher channel efficiency than traditional methods. Besides of experimental results, analytical models of the proposed coloring based scheduling are also provided in chapter 3.

Finally, in chapter 4, issue of complex WBAN priorities are further analyzed and suggested solution is provided. Proposed QoS controls simultaneously consider three different priorities: (i) intrinsic data priority, (ii) emergent data priority, and (iii) user priority. Experiment results show that the proposed method not only properly deals the complex user priorities, it can also support high user capacity than that without considering the interference from inter-WBANs.

## 5.2 Future Works

Based on above results of this study, some future works are suggested:

**Establishing Multiuser WBAN channel model**

This study only applies simple shading models for the calculation of interference. In real world, multiple human bodies may cause very complicated shadowing effect and hence the proposed methods in this study might need further adjustments. However, most existing WBAN channel models can only calculate the attenuation caused by one human body [56]. The bottleneck of multi-user channel model study is numerous combinations of input parameters. Different user positions, angles, gestures, and body shapes all affect attenuation level. Furthermore, there are many imperfect effects on reflection, scattering, radiation, and coupling of human body, which make the rule of attenuation hard to be summarized and simplified. To our best understanding, existing channel models can consider only up to two human bodies [57]. It is still complicated and far from

the n-user model required in our study. For this reason, radio attenuation due to human body is temporally ignored in this study and hence the multi-user WBAN resource allocation problem can be more focused.

**Integrating medical and legal knowledge for WBAN QoS control**

In the proposed multi-WBAN QoS control, the real priorities between various vital signals and alarm threshold (priority enhance) still relies on medical experiences. Also, a complete WBAN QoS might be accompanied with dynamic signal quality scheme. For example, with very limited wireless resource, an ECG sensor might optionally switch to lower resolution mode. However, what is the limit of the degradation of signal quality? The answer may vary with difference target syndromes. This relies on more practices and understanding of working flow of medical scenes. Finally, will the priority controls between involve legal issues? Since priority scheme implies sacrifices among measured signals in some critical situations. The prioritizing procedure may involve human life. Hence, related designs might involve technology, medical, and legal knowledge. Of course, backup procedure may be necessary in such sensitive applications.

# Bibliography


[1] M. Patel, and W. Jianfeng, "Applications, challenges, and prospective in emerging body area networking technologies," *IEEE Wireless Communications,* vol. 17, no. 1, pp. 80-88, Feb, 2010.

[2] M. Chen, S. Gonzalez, A. Vasilakos, H. Cao, and V. C. Leung, "Body Area Networks: A Survey," *Mobile Networks and Applications,* vol. 16, no. 2, pp. 171-193, 2011.

[3] I. F. Akyildiz, W. L. Su, Y. Sankarasubramaniam, and E. Cayirci, "A survey on sensor networks," *IEEE Communications Magazine,* vol. 40, no. 8, pp. 102-114, Aug, 2002.

[4] S. M. Jiang, Y. D. Liu, Y. M. Jiang, and Q. G. Yin, "Provisioning of adaptability to variable topologies for routing schemes in MANETs," *IEEE Journal on Selected Areas in Communications,* vol. 22, no. 7, pp. 1347-1356, Sep, 2004.

[5] D. Niyato, E. Hossain, and S. Camorlinga, "Remote patient monitoring service using heterogeneous wireless access networks: Architecture and optimization," *Ieee Journal on Selected Areas in Communications,* vol. 27, no. 4, pp. 412-423, 2009.

[6] J. Misic, and V. B. Misic, "Bridging Between IEEE 802.15.4 and IEEE 802.11b Networks for Multiparameter Healthcare Sensing," *Ieee Journal on Selected Areas in Communications,* vol. 27, no. 4, pp. 435-449, May, 2009.

[7] S. Garawi, R. S. H. Istepanian, and M. A. Abu-Rgheff, "3G wireless communications for mobile robotic tele-ultrasonography systems," *Ieee Communications Magazine,* vol. 44, no. 4, pp. 91-96, Apr, 2006.

[8] G. Rung-Hung, "Modeling the slotted nonpersistent CSMA protocol for wireless access networks with multiple packet reception," *Communications Letters, IEEE,* vol. 13, no. 10, pp. 797-799, 2009.

[9] B. J. B. Fonseca Jr, "An augmented graph-based coloring scheme to derive upper bounds for the performance of distributed schedulers in CSMA-based mobile ad hoc networks," in *International Wireless Communications and Mobile Computing Conference,* Vancouver, BC, Year, pp. 761-766.

[10] P. Joseph, H. Jason, and C. David, "Versatile low power media access for wireless sensor networks," in *Proceedings of the 2nd international conference on Embedded networked sensor systems,* Baltimore, MD, USA, 2004, pp.

[11] Z. Jialiang, S. C. Liew, and F. Liqun, "On fast optimal STDMA scheduling over fading wireless channels," in *2009 IEEE INFOCOM. 28th International Conference on Computer Communications,* Rio de Janeiro, Brazil, Year, pp. 1710-1718.

[12] H. Lee, D. C. Cox, and Ieee, "A FULLY-DISTRIBUTED CONTROL TIME SLOT ASSIGNMENT PROTOCOL FOR LARGE WIRELESS MESH NETWORKS," in *IEEE Military Communications Conference (MILCOM 2008),* San Diego, CA, Year, pp. 4131-4138.

[13] IEEE 802.15 WPAN Task Group 6 Body Area Networks, "15-08-0644-09-0006-tg6 technical requirements document," 2008.

[14] W. Ye, J. Heidemann, and D. Estrin, "An energy-efficient MAC protocol for wireless sensor networks," in *INFOCOM,* 2002, pp. 1567- 1576.

[15] T. Y. Lin, Y. K. Liu, and Y. C. Tseng, "An improved packet collision analysis for

multi-Bluetooth piconets considering frequency-hopping guard time effect," *Ieee Journal on Selected Areas in Communications,* vol. 22, no. 10, pp. 2087-2094, Dec, 2004.
[16] A. El-Hoiydi, "Interference between Bluetooth networks - Upper bound on the packet error rate," *IEEE Communications Letters,* vol. 5, no. 6, pp. 245-247, Jun, 2001.
[17] FCC, "Wireless Medical Telemetry," 2000.
[18] B. De Silva, A. Natarajan, and M. Motani, "Inter-user interference in body sensor networks: Preliminary investigation and an infrastructure-based solution," in *6th International Workshop on Wearable and Implantable Body Sensor Networks,* Berkeley, CA, 2009, pp. 35-40.
[19] S. H. Cheng, and C. Y. Huang, "Power model for wireless body area network," in *IEEE Biomedical Circuits and Systems Conference,* Baltimore, 2008, pp. 1-4.
[20] S. H. Cheng, M. L. Liu, and C. Y. Huang, "Radar based network merging for low power mobile wireless body area network," in *4th International Symposium on Medical Information and Communication Technology,* Taipei, 2010, pp.
[21] I. Howitt, "Mutual interference between independent Bluetooth piconets," *IEEE Transactions on Vehicular Technology,* vol. 52, no. 3, pp. 708-718, May, 2003.
[22] S. Gandham, M. Dawande, and R. Prakash, "Link scheduling in wireless sensor networks: Distributed edge-coloring revisited," *Journal of Parallel and Distributed Computing,* vol. 68, no. 8, pp. 1122-1134, Aug, 2008.
[23] S. Ramanathan, "A unified framework and algorithm for channel assignment in wireless networks," *Wireless Networks,* vol. 5, no. 2, pp. 81-94, Mar, 1999.
[24] D. B. West, *Introduction to Graph Theory,* 2 ed., Prentice Hall, 2000.
[25] C. Zhu, and M. S. Corson, "A five-phase reservation protocol (FPRP) for mobile ad hoc networks," *Wireless Networks,* vol. 7, no. 4, pp. 371-384, Aug, 2001.
[26] A. Bjorklund, T. Husfeldt, and M. Koivisto, "Set partitioning via inclusion-exclusion," *SIAM Journal on Computing,* vol. 39, no. 2, pp. 546-563, Jul, 2009.
[27] Ö . Johansson, "Simple distributed Δ+1-coloring of graphs," *Information Processing Letters,* vol. 70, no. 5, pp. 229-232, Jun, 1999.
[28] K. Kothapalli, C. Scheideler, M. Onus, and C. Schindelhauer, "Distributed coloring in O( radic (log n)) bit rounds," in *20th International Parallel and Distributed Processing Symposium,* Rhodes Island, Greece, 2006, pp. 10.
[29] Y. Métivier, J. M. Robson, N. Saheb-Djahromi, and A. Zemmari, "About randomised distributed graph colouring and graph partition algorithms," *Information and Computation,* vol. 208, no. 11, pp. 1296-1304, 2010.
[30] R. M. Corless, G. H. Gonnet, D. E. G. Hare, D. J. Jeffrey, and D. E. Knuth, "On the Lambert W Function," *Advances in Computational Mathematics,* vol. 5, pp. 329-359, 1996.
[31] D. A. Grable, and A. Panconesi, "Nearly optimal distributed edge coloring in O(log log n) rounds," *Random Structures & Algorithms,* vol. 10, no. 3, pp. 385-405, May, 1997.
[32] C. T. Chou, J. Del Prado Pavon, and S. Shankar N, "Mobility support enhancements for the WiMedia UWB MAC protocol," in *2nd International Conference on Broadband Networks,* Boston, MA, Year, pp. 213-219.
[33] V. Tolety, "Load reduction in ad hoc networks using mobile servers," Master's thesis, Dept. of Mathematical and Computer Sciences, Colorado School of Mines, Colorado, 1999.
[34] T. Camp, J. Boleng, and V. Davies, "A survey of mobility models for ad hoc network research," *Wireless Communications & Mobile Computing,* vol. 2, no. 5, pp. 483-502, Aug, 2002.
[35] M. A. Ameen, A. Nessa, and K. Kyung Sup, "QoS Issues with Focus on Wireless Body Area Networks," in *Third International Conference on Convergence and Hybrid Information*

*Technology*, 2008, pp. 801-807.
[36] J. S. Yoon, A. Gahng-Seop, J. Seong-Soon, and M. J. Lee, "PNP-MAC: preemptive slot allocation and non-preemptive transmission for providing QoS in body area networks," in *IEEE Consumer Communications and Networking Conference (CCNC)*, Las Vegas, NV, 2010, pp. 1-5.
[37] F. Masse, and J. Penders, "Quality-of-service in BAN: PER reduction and its trade-offs," in *International Conference on Body Sensor Networks (BSN)*, Singapore, Singapore, 2010, pp. 261-266.
[38] C. Huasong, S. Gonza lez-Valenzuela, and V. C. M. Leung, "Employing IEEE 802.15.4 for Quality of Service Provisioning in Wireless Body Area Sensor Networks," in *International Conference on Advanced Information Networking and Applications*, Perth, WA, Australia, 2010, pp. 902-909.
[39] K. A. Ali, J. H. Sarker, and H. T. Mouftah, "Urgency-Based MAC Protocol for Wireless Sensor Body Area Networks," in *International Conference On Communications Workshops*, Capetown, South Africa, 2010, pp. 1-6.
[40] H. Su, and X. Zhang, "Battery-dynamics driven tdma mac protocols for wireless body-area monitoring networks in healthcare applications," *IEEE Journal on Selected Areas in Communications*, vol. 27, no. 4, pp. 424-434, May, 2009.
[41] B. Otal, L. Alonso, and C. Verikoukis, "Novel QoS scheduling and energy-saving MAC protocol for body sensor networks optimization," in *Proceedings of the ICST 3rd international conference on Body area networks*, Tempe, Arizona, 2008, pp. 1-4.
[42] Z. Gang, L. Jian, W. Chieh-Yih, M. D. Yarvis, and J. A. Stankovic, "BodyQoS: adaptive and radio-agnostic QoS for body sensor networks," in *IEEE INFOCOM*, Phoenix, AZ, 2008, pp. 1238-1246.
[43] X. Jiang, and I. Howitt, "Multi-domain WLAN load balancing in WLAN/WPAN interference environments," *IEEE Transactions on Wireless Communications*, vol. 8, no. 9, pp. 4884-4894, Sep, 2009.
[44] B. Nazir, and K. Zia, "QoS aware interpiconet scheduling in Bluetooth Scatternet (QIPS)," in *Third International Conference on Emerging Technologies*, Islamabad, Pakistan, 2007, pp. 68-73.
[45] K. Maalaoui, and L. A. Saidane, "FP/EDF versus FP/FIFO local scheduling and probabilistic QoS guarantees in a Bluetooth piconet," in *21st International Conference on Advanced Networking and Applications Workshops/Symposia*, Los Alamitos, 2007, pp. 905-910.
[46] S. Saha, and M. Matsumoto, "An Inter-Piconet Scheduling Algorithm for Bluetooth Scatternets," in *International Conference on Internet and Web Applications and Services/Advanced International Conference on Telecommunications*, 2006, pp. 24-24.
[47] N. Golmie, "Bluetooth Dynamic Scheduling and Interference Mitigation," *Mobile Networks and Applications*, vol. 9, no. 1, pp. 21-31, Feb, 2004.
[48] F. Cuomo, T. Melodia, and I. F. Akyildiz, "Distributed self-healing and variable topology optimization algorithms for QoS provisioning in scatternets," *IEEE Journal on Selected Areas in Communications*, vol. 22, no. 7, pp. 1220-1236, Sep, 2004.
[49] C. Wei-Peng, and J. C. Hou, "Provisioning of temporal QoS in Bluetooth networks," in *IEEE Conference on Mobile and Wireless Communications Networks*, Stockholm, Sweden, 2002, pp. 389-393.
[50] C. Y. Huang, M. L. Liu, and S. H. Cheng, "WRAP: A Weighted Random Value Protocol for Multiuser Wireless Body Area Network," in *International Symposium on Information Theory and its Applications and International Symposium on Spread Spectrum Techniques and Applications*, Taichung, Taiwan, 2010, pp. 116-119.

[51] S. Ullah, B. Shen, S. M. Riazul Islam, P. Khan, S. Saleem, and K. Sup Kwak, "A Study of MAC Protocols for WBANs," *Sensors,* vol. 10, no. 1, pp. 128-145, 2009.
[52] S. Ullah, H. Higgins, B. Braem, B. Latre, C. Blondia, I. Moerman, S. Saleem, Z. Rahman, and K. Kwak, "A Comprehensive Survey of Wireless Body Area Networks," *Journal of Medical Systems*, pp. 1-30, 2010.
[53] S. J. Marinkovic, E. M. Popovici, C. Spagnol, S. Faul, and W. P. Marnane, "Energy-Efficient Low Duty Cycle MAC Protocol for Wireless Body Area Networks," *IEEE Transactions on Information Technology in Biomedicine,* vol. 13, no. 6, pp. 915-925, 2009.
[54] S. Ullah, and K. Kwak, "An Ultra Low-power and Traffic-adaptive Medium Access Control Protocol for Wireless Body Area Network," *Journal of Medical Systems*, pp. 1-10, 2010.
[55] L. Bao, and J. J. Garcia-Luna-Aceves, "A new approach to channel access scheduling for ad hoc networks," in *7th Annual International Conference on Mobile Computing and Networking, July 16, 2001 - July 21, 2001*, Rome, Italy, Year, pp. 210-220.
[56] K. Y. Yazdandoost, *IEEE 802.15-08-0780-07-0006 Channel Model for Body Area Network*, 2009.
[57] G. Koutitas, "Multiple human effects in body area networks," *Ieee Antennas and Wireless Propagation Letters,* vol. 9, no. Compendex, pp. 938-941, 2010.

# List of Publications

**Key Technology One: Multiuser Inter WBAN Scheduling**

**Publications:**

1. ShihHeng Cheng,ChingYao Huang, "Power model for wireless body area network," *Biomedical Circuits and Systems Conference*, Baltimore, MD, Nov, 20-22, 2008.
2. ShihHeng Cheng,MeiLing Liu, ChingYao Huang, "Radar Based Network Merging for Low Power Mobile Wireless Body Area Network," *4th International Symposium on Medical Information and Communication Technology*, Taipei, Mar, 22-25, 2010.
3. C. Y. Huang, M. L. Liu, and S. H. Cheng, "WRAP: A Weighted Random Value Protocol for Multiuser Wireless Body Area Network," in International Symposium on Information Theory and its Applications and International Symposium on Spread Spectrum Techniques and Applications, Taichung, Taiwan, 2010, pp. 116-119.
4. ShihHengCheng,ChingYao Huang, "Coloring-Based Inter-WBAN Scheduling for Mobile Wireless Body Area Network," IEEE Transactions on Parallel and Distributed Systems, vol. 99 (Accepted; Early Access)
5. ShihHeng Cheng, Chun Chen Tu, and ChingYao Huang, "RACOON: A Multiuser QoS design for Mobile Wireless Body Area Networks", Journal of Medical Systems, vol. 35, no. 5, pp. 1277-1287, 2011

**Standard Contributions:**

1. ShihHeng Cheng, ChingYao Huang, "Network Merging : Design Strategies of An Ultra Low Power and High Reliability MAC (15-09-0227-00-0006)," *Standard Meeting: IEEE 802.15 TG6 Wireless Body Area Network (WBAN) 2009*, March 9-13, Vancouver.

**Patents:**

1. 黃經堯, 程士恒, "多無線網路間的封包碰撞避免技術, Method for packet collision avoidance between multiple wireless network," 2008, JP issued; TW, US, CN Pending.

**Key Technology Two: WBAN Channel Measurement and Modeling**

**Publications:**

1. ChingYao Huang,JhihCiangCai, ShihHeng Cheng, Wei Chou, "A Time Based Two-State Channel Model for Dynamic Wireless Body Area Networks," *4th International Symposium on Medical Information and Communication Technology*, Taipei, Mar, 22-25, 2010.

**Standard Contributions:**

1. JhihCiangCai, ShihHeng Cheng, ChingYao Huang, "MAC Channel Model for WBAN (15-09-0562-00-0006)," *Standard Meeting: IEEE 802.15 TG6 Wireless Body Area Network (WBAN) 2009*, July 12-17, San Francisco

**Key Technology Three: Applications of WBANs**

**Patents:**

1. 黃經堯, 程士恒, “防盜用圖章, Method and Apparatus for Anti-steal Stamp,” 2008, TW Patent (Pending).
2. 李鎮宜, 陳瑞杰, 黃經堯, 游瑞元, 莊子宗, 程士恒, “緊急醫療用無線心電貼片, First Aid Wireless ECG Pad,” 2010 (Pending).
3. 程士恒, “心電訊號處理裝置,” 2012, TW Patent (Pending)

**Competition:**

1. 李鎮宜, 黃經堯, 宋偉豪, 程士恆, 李曜, “防盜用圖章,” 2008 ARM Code-O-Rama 設計大賽亞軍.